Experimental investigations on rapid filling of empty pipelines

Report UMCEE-05-01

Jose G. Vasconcelos
Steven J. Wright
and Mokhtar Guizani

University of Michigan
Department of Civil and Environmental Engineering
Ann Arbor, Michigan

January 3, 2005

Summary

The filling of an initially empty pipeline is a problem of great interest due to the many practical applications in hydraulics. Several potential problems may arise during the filling process, especially in rapid filling conditions. Among these problems, one includes water-hammer caused by the rapid ventilation of air pockets present within the pipes (Wylie and Streeter, 1993) and pressure surges. Investigations on this problem have yielded different numerical models that attempt to describe the filling process. Some simplifying assumptions were introduced in these models, including the existence of a vertical interface that would characterize the flow advance. However, it is unclear whether this is a reasonable assumption, particularly in cases when the upstream pressure head on the supply reservoir is relatively low. The importance of this issue is related to the development of air pockets in the system during filling events. This study presents the results of a systematic investigation of the shape and behavior of the inflow front caused by the rapid filling of an initial empty pipeline. Nine different configurations of initial pressure heads at the supply reservoir and pipe slopes were tested. For each run the shape of the front was recorded with the aid of a digital camera, and a piezo-resistive pressure transducer was used to monitor the pressure variation during the front passage. The results were compared with the predictions of two different types of numerical models to describe the filling process. It was confirmed that in some conditions the inflow front cannot close the pipe cross section, thus invalidating the assumption of vertical interface fronts.

Contents

Chapter 1

Introduction and Objectives

While liquid flow in pipelines is of great interest in hydraulics, some transient flow conditions remain poorly understood to date. Among such conditions, one includes the flow initiation in initially empty pipelines. This is a situation that happens in a number of practical applications in hydraulics, including the filling of water mains and the start-up of pumping lines.

The pipeline filling process can be either gradual or rapid. In the latter case there is the potential for problems to develop caused generally by the entrapment of air pockets within the pipes. These problems include water-hammer type of pressures caused by sudden ventilation of these air pockets and pressure surges caused by air pocket compression. In this context, it is very important to understand the causes of air pocket generation. One speculates that a possible cause is related to cases when the inflow front does not fill the entire pipe cross section during the pipeline filling process, in which case it is possible that air pockets will be left entrapped behind the water front. Therefore it is important to study the shape of the inflow front.

Preliminary experiments at the fluids laboratory at the University of Michigan confirmed this possibility. In those experiments, water supplied by an large upstream tank was admitted into an 94 mm diameter acrylic pipeline. In some cases, particularly when the water level in the supply tank was less than 4 times the pipe diameter, it was noticed that the inflow front did not fill the pipe cross section, leaving air behind as it advanced through the system.

The issue becomes more important when existing investigations are considered. These investigations, exemplified by the works by Liou and Hunt (1996); Izquierdo et al. (1999) and Zhou et al. (2002) resulted in numerical models constructed around the assumption that the inflow front can be represented by a vertical interface. This assumption is a simplification of the actual problem, since the shape of the inflow front would be dependent on factors such as the cross section geometry, pipe slope, friction, among others. However, the vertical front assumption may be compromised in cases when the pipe cross section is not totally filled by the inflow front.

This report has the following objectives:

- Describe experiments to study the shape of the inflow front for different cases of rapid filling of empty pipelines
- Assess the validity of the vertical front interface assumption
- Compare the experimental results with predictions of numerical models proposed by Liou and Hunt (1996) and Vasconcelos et al. (2005).

The report is structured as follows. Chapter 2 discusses the previous investigations on this theme, focusing on the criteria for the pipe to flow full and numerical model development. Chapter 3 presents the experimental methodology followed in this investigation. Chapter 4 presents the experimental results, the comparison with the numerical predictions and the analysis of these results. Chapter 5 presents the conclusions of this work.

Chapter 2

Previous investigations

2.1 Criteria for full pipeline flow

The general description of the flow initiation in an empty pipeline can be visualized as a sequence of events in which different processes control the flow behavior. When the inflow valve is just opened, the inflow rate is zero and the inflow front is not well defined. Observations of the flow behavior following a sudden valve opening show that the front shape is complex both in space and in time. Following the opening, a rapid flow acceleration is observed and the velocity reaches a maximum. As the flow advances in the pipe, frictional losses will cause a reduction in the velocity, and consequently in the conveyed inflow (Liou and Hunt, 1996).

However, prior to the discussion of modeling the pipeline filling problem, one needs to be careful in putting the discussion of the criteria for the pipeline flow full state in the proper context. In other words, it is necessary to determine the conditions in order to the inflow be conveyed as a full pipe flow. This issue is crucial to determine the validity of some numerical models of the problem, particularly the models that rely on the assumptions of a vertical front interface. There are at least two different mechanisms that could determine whether the pipeline filling will occur in closed pipe mode. One is based on the minimum conveyance required for the pressurized pipe flow, while the other is based on a minimum velocity that the flow would need to avoid the intrusion of an air cavity. In the latter case, the problem would require the inclusion of the air phase in the analysis.

In either case, the first interaction between water and air phases occur immediately after the flow initiation. The description of the water flow in this initial stage, if possible, would require a transient, three-dimensional, two-phase flow framework particular for the type of flow geometry (e.g. valve type). This is too complex, and thus avoided in most hydraulic applications by assuming that the water phase will displace the air. This initial phase is of short duration, and is followed by the development of a well-defined inflow front shortly after the inflow enters the pipeline.

The first mechanism that would dictate whether the pipe will flow full following the rapid acceleration phase is based on the conveyance criteria. In this criteria, if the inflow is too small, the empty pipeline would be able to convey the flow as a free-surface flow. Pressurized flow would not occur at the inflow front as air would still exist on the upper portion of the pipe already conveying water. The accumulation of water at the low points of the pipeline could result in the entrapment of air pockets in the pipeline, which is (as explained) a potential source of operational problems. On the other hand, if the inflow rate is larger than the capacity of the pipeline to convey the inflow as an open channel, pressurized flow would result. Because behind the pressurization front there is

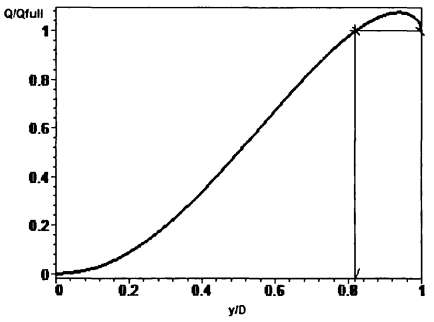

Figure 2.1: Rating curve for steady uniform discharge in circular pipes, with fixed Manning coefficient and a given energy slope.

mostly water, the possibility for air pocket entrapment is reduced.

Unfortunately, this issue is complicated by the geometric characteristics of the circular cross section. Figure 2.1 shows, for a fixed Manning coefficient and a given energy slope, the theoretical ratio between the inflow rate at a given non-dimensional depth y/D in the pipe and the inflow rate when the pipe flow, as an open channel, is flowing full (e.g. piezometric head at the pipe crown). One notices that the geometric characteristics of the circular cross section creates the conditions of maximum conveyance when y/D=0.938. Moreover, when the inflow depth is between y/D=0.82 and y/D=1, there is no unique depth in which the inflow could be conveyed. In other words, the same inflow could be conveyed by two different piezometric heads, one corresponding a to free-surface flow, the other to pressurized flow, characterizing a potentially unstable condition (Yen, 2001). Chow (1973) points to a earlier study that the friction coefficient n varies with the y/D ratio. This variability reduces the problem of non-uniqueness for the depth to a given flow to a point the practically the maximum discharge would occur at y/D=1, or full pipe depth. However, no recent studies have been conducted to confirm the influence of y/D on the Manning coefficient, and the actual flow behavior near full pipe conditions is not well understood.

The second possible mechanism to determine whether the pipe will flow full checks the possibility of air intrusion on the pipe as the inflow advances on the pipe. This mechanism is related to a "minimum velocity" criteria required to avoid the intrusion of air pockets on the water flow, and was used by Liou and Hunt (1996). Zukoski (1966) investigations determined that the speed of air pockets (celerity) in horizontal circular pipelines is $0.54\sqrt{gD}$. Thus, if the water flow velocity is larger than this value, there would be no air intrusion and the pipe would flow full. Along the same lines, a study by Wisner et al. (1975) pointed to a minimum velocity to assure the removal of air pockets from water lines that depended on the air pocket celerity and the pipeline angle with the horizontal.

To illustrate this mechanism, Townson (1991) proposed the following problem, illustrated in figure 2.2. A 1 km long, 2 x 2 m square cross section tunnel is initially fully pressurized with a piezometric head of 10 m with a downstream valve closed causing a no-flow condition. Following a sudden opening of the gate, in a finite amount of time, an air intrusion will form on the top of the tunnel and advance toward the upstream reservoir. After some time the flow velocity increases to a point that stops the intrusion progression. As the inflow velocity becomes larger than the celerity of the air cavity, the intrusion will stop and the flow will remove the air from the pipeline.

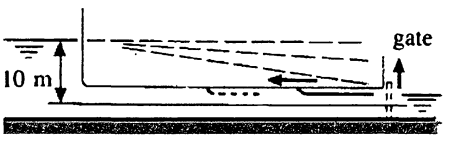

Figure 2.2: Problem presented by Townson (1991) to illustrate the intrusion of an air pocket upon gate opening in a 1 km long, 2x2 m square cross section tunnel.

The question now is what mechanism is more appropriate to determine whether air intrusion occurs. It is anticipated that the conveyance criteria would be more appropriate to the problem of rapid filling of an empty pipeline. This is because the intrusion velocity criteria would require a cross section initially filled with water to be applicable. One example is the flow initiation of an initially filled pipeline as proposed by Townson (1991). This assumption needs, however, experimental confirmation for other cases and appears not to have been previously studied.

Although the problem of sudden initiation of liquid flow into a initially empty pipeline has had little experimental study into the nature of the air-water interface, the somewhat analogous problem of density intrusions has been subject of considerable investigation. One important example is that of salt water intrusion into freshwater; because the low density difference in most applications compared to that of between air and water, the phenomena evolve more slowly and it is possible to make quantitative measurements more readily. Considering the release of salt water into a quiescent fresh water conduit, he salt water advances as a well defined front and Benjamin (1968) suggested that this and the air intrusion problem were analogous. However, in the case of a flowing fresh water system the well defined intrusion front vanishes and the so-called salt water wedge develops (reference?). The location of the wedge is controlled by friction and therefore is related to the conveyance criterion discussed above. Paez (???) on the basis of observations of salt water intrusion into flowing fresh water systems demonstrated that well-defined intrusion fronts do not form when the salt water intrusion velocity relative to the fresh water flow is less than zero. This lends support to the concept that interaction at the air-water interfaces at rapidly advancing front is not controlled by the same processes as air intrusion into a nearly stagnant water column.

A simple comparison between the two criteria is promoted here. The conveyance criteria depends on several factors, such as the flow energy slope, pipe diameter and rugosity. On the other hand, the velocity criteria depends only in the pipe diameter. A comparison is conducted by equating the air cavity celerity required by the velocity based criteria with a velocity provided by the Manning equation. The velocity from this open-channel equation is calculated for the case when the pipe is flowing full, so that the hydraulic radius is D/4. This is assumed the minimum speed (for given values of n and S_f) for the pipe to flow in the pressurized regime according to the conveyance criteria. Equating these two expressions we have:

$$\frac{1}{n}(D/4)^{2/3}\sqrt{S_f} = K\sqrt{gD} \tag{2.1}$$

In the above equation, n is the Manning coefficient, D is the pipe diameter, S_f is the energy slope, g is the gravity acceleration and K is a general proportionality coefficient for the air pocket celerity that depends on the viscosity, surface tension and pipe slope. Assuming K = 0.54 as suggested by Zukoski (1966) for horizontal pipes, the energy slope requirement that would make

the velocity from conveyance based criteria larger than then the one from the velocity based criteria is:

$$S_f >= 18.156\frac{n^2}{D^{1/3}} \tag{2.2}$$

For a 1.0 m diameter tunnel, with Manning coefficient of 0.01, the value for S_f should be greater than 0.182% so that the conveyance criteria velocity is the larger one. Equation 2.1 helps to illustrate that each criteria can yield much different velocity predictions. In the following chapters the experimental results are compared to each one of these criteria to assess their applicability.

2.2 Numerical modeling of the pipeline filling problem

Numerical models have been developed to simulate rapid pipeline filling along with experimental investigations to validate such models. Liou and Hunt (1996) presented a numerical model based on the rigid column assumption which aims to describe the filling of a undulating pipeline. The numerical model solved a non-linear ordinary differential equation that described the evolution of the column velocity with time. Because of the rigid column model used, the advancing water front interface was assumed vertical. To validate this assumption, the authors used the velocity based criteria, mentioned in the previous section. Experimental investigations were conducted in a PVC pipe of 2.29 cm diameter and 6.66 m long connected to a large upstream reservoir by means of a quarter-turn valve. Upon sudden opening of the valve, indirect measurements of the velocity indicated a rapid acceleration of the water column within the pipe. As the column progressed, despite the downward slope of the pipe, the velocity of the column decreased due to frictional energy losses.

The study by Izquierdo et al. (1999) dealt with the undulating pipeline filling problem when air pockets are initially entrapped by water accumulated in the pipeline low points, referred in the article as water blocking columns. As a consequence, the proposed numerical model included a more complex set of equations to describe both the position and velocity of the advancing front, the air pocket pressures and the position, size and velocity of the water blocking columns. The model formulation required the assumption of well-defined air-water interfaces. Thus, this study disregarded the possibility of the pipeline section to convey the inflow in a open-channel flow regime.

In summary, there are few numerical models that aim to describe the pipeline filling problem based on the rigid column assumption. These models assume that a vertical interface separates the inflow front from the air phase that is present in the pipe. In the Liou and Hunt (1996) model, the full pipe flow criteria that was used was based on a minimum velocity required to prevent the intrusion of an air cavity. No experimental investigation was directed to assess the validity of the vertical interface assumption or the air intrusion criteria. Those are the main goals of the investigation presented in this report.

Chapter 3

Methodology

3.1 Experimental apparatus

The experiments were conducted in the fluids laboratory at the University of Michigan. The apparatus, illustrated in figure 3.1, was consisted of the following components:

- Upstream metallic head tank, with cross section area of 2.96 m^2;
- Fast-opening rubber seal connecting the tank and the pipeline, which permitted the manual start of the inflow;
- Acrylic pipeline, 14.2 m long and 0.094 m diameter, connected with the upstream head tank with a plunge valve (see figure 3.2);
- The pipeline was mounted inside a 15 m long flume, and was supported on wooden spacers;
- Piezoresistive pressure transducer, manufactured by ENDEVCO model 8510B-1, (1 PSIg) located at 12.6 m downstream from the upstream end;
- Data acquisition board, manufactured by National Instruments, model DAQ-Pad MIO-16XE-50, connected to a laptop computer to collect the transducer output;
- Digital camcorder with 30 frames per second speed, located at the same station as the pressure transducers. In some experiments two digital camcorders were used simultaneously. The recording region was between 11.4 m and 12.6 m from the upstream end. When the second digital camcorder was used, the recording region was between 10.2 m and 11.4 m from the upstream end.
- Downstream tank, circular with 0.19 m diameter located in the end of the pipeline, which collected the flow after the front shape was recorded.

3.2 Experimental variables and procedure

Two different experimental variables were systematically tested in the experiments. The first one was the pipeline slope, chosen because the previous investigations considered the effect of the

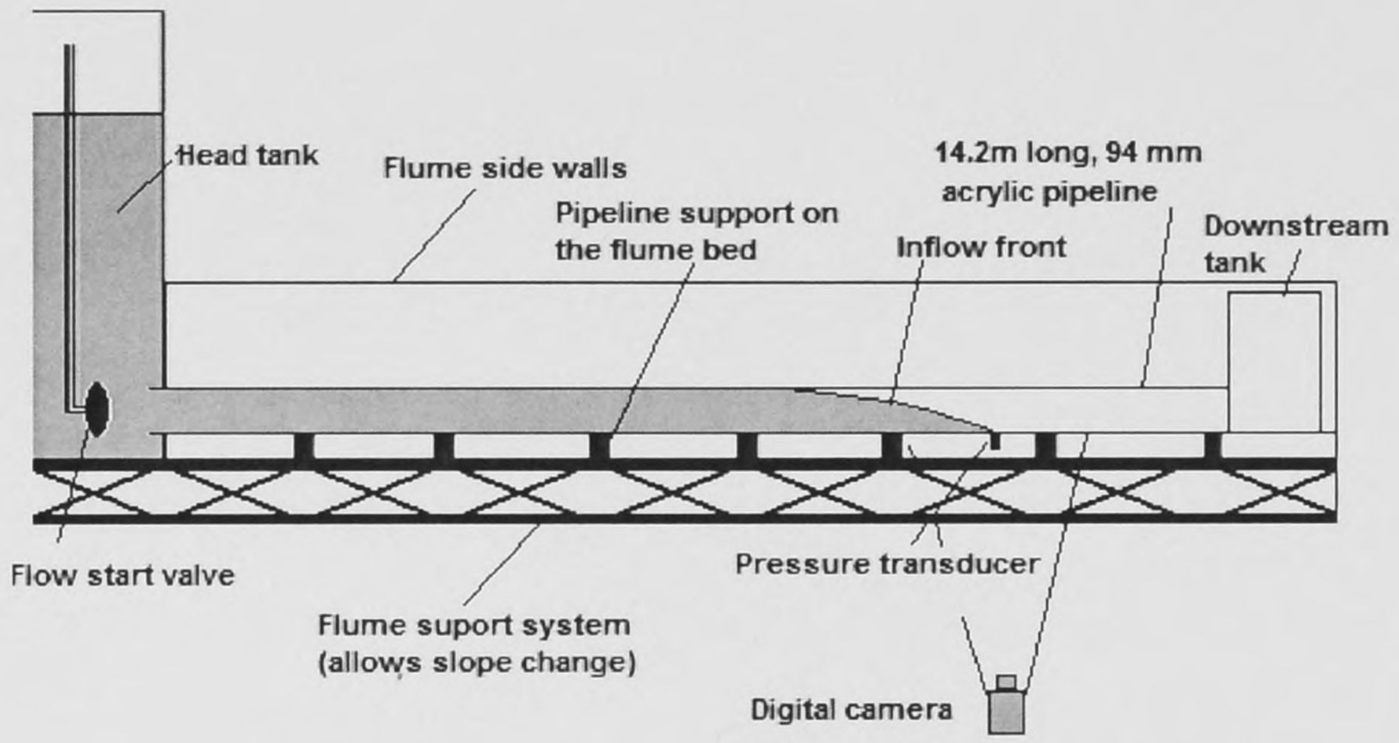

Figure 3.1: Schematic of the experimental apparatus

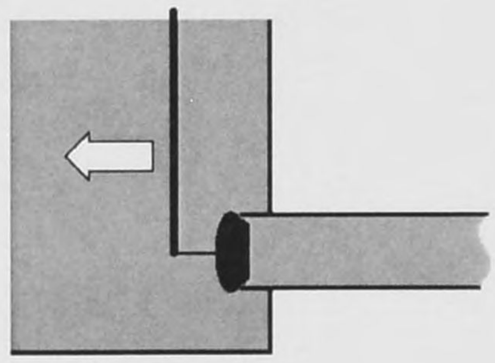

Figure 3.2: Schematic of valve that controlled the inflow at the upstream end of the pipeline

pipeline slope in the filling process. Three different slopes were used in this investigation: horizontal, upward (adverse) 0.40% and downward 1.02%. The slopes were limited by the ability to adjust the slope of the tilting flume.

The second experimental variable used in this investigation was the upstream pressure head in the tank before the experiment started. It was anticipated that by changing this pressure head different inflow rates could be obtained in the pipe, which would help to determine whether the conveyance criteria is really applicable to the pipeline filling problem. In total, nine different conditions were tested, and Table 3.1 shows the range of conditions included in this investigation.

Table 3.1: Experimental variables used in the investigation

Parameter	Range tested
Pipeline slope	Horizontal, 1.02% downward, 0.40% upward
Upstream pressure head	3.9, 6.6 and 9.2 times pipe diameter

The experiments were divided into two phases, each with an specific objective. The first phase of experiments aimed to record the shape of the advancing front with two digital camcorders recording images at adjacent sections of the pipeline. This arrangement was required because preliminary experiments indicated that the front would spread over more than 10 pipe diameters. Each camcorder was located to provide a field of view 1.0 m wide. In these experiments the pressure transducer was also used to measure the pressure as the front advanced.

The second phase of the experiments aimed to assess the effect of the pipe slope in the front advance and the filling process. For those experiments, the pressure transducers where also used to track the pressure at the front during the passage of the front. In some cases the spreading of the front was much larger than the 2.0 m field of view achieved with two camcorders. Technical difficulties prevented the use of two cameras simultaneously for the cases when the slope was either upward or downward. Thus, in order to obtain trajectory information for the 2.0 m stretch of the pipeline, pairs of identical experiments were conducted, one with the camera placed at the upstream recording location, and the other at the downstream location. While this arrangement was not ideal, it provided an estimate of the front history for the sloped cases.

Generally, the experimental procedure was the following:

1. The pipe was set in the desired slope by adjusting the slope of the flume;
2. The fast-opening seal isolating the pipeline from the head tank was closed. Then water was admitted in the head tank raising the level to the desired initial level;
3. The water present in the pipeline was drained/pumped out;
4. In sequence, the digital camera(s), then the pressure transducer were started before the flow start. In this way, the camera could record the time lag between the transducer start and the flow start;
5. The flow was started by pulling rapidly the seal off the pipeline upstream end, initiating the pipeline filling;
6. Some time after the inflow front passed the recording location, the camera and the transducer were stopped;

7. Each experimental condition was repeated three times to assure repeatability.

It is acknowledged that this experimental set-up is a simplification from the real problem of pipeline flows. These simplifications include the quick valve opening, the pipeline comprised by a single segment with one slope and the pipeline length. Yet, this set-up retains the essential elements of actual problems.

3.3 Data analysis procedure

Because of the lack of previous investigations, no existing concepts on how to characterize the shape of the advancing front were available. A criteria was developed and applied to each experimented condition. Preliminary experimental observations indicated that the inflow front shape was not vertical, but instead it resembled a wedge. To characterize this front shape a simplistic approach was selected, in which the front shape was represented using three points. The first point is located in the where the front touches the pipe bottom, the second where the front depth equalled half of the pipe depth, and the third where the front touched the pipe crown. These points are referred herein as front features.

The trajectory of each front feature was plotted against time, showing for instance how wide the front was and whether this width changed with time. In some cases, as it will be discussed later, feature 3 (on the pipe crown) could not be recorded with the movies because the inflow front did not reach the pipe crown as it traveled past the digital camera recording section. Because the flow start was manual, small differences (around 0.5 s) were possible, which affect the location of the inflow front. This is visible in the trajectory plots, since for different repetitions the trajectories are not coincident. By an averaging of these trajectories over the three repetitions, the effect of different flow start times can be minimized.

The movie results were also compared with the output from the transducers, which recorded the pressure variation during the filling process at the 12.6 m station. Although the pressure is not hydrostatic at the vicinity of the moving front, three pressure heads points corresponding to 0, D/2 and D (D is the pipe diameter) were plotted along with the arrival time of the three front features at the 12.6 m station. This provided an insight on how the depths recorded from the movies compare to the pressure transducer results.

Chapter 4

Results and Data Analysis

4.1 Shape of the inflow front for horizontal pipelines

These experiments aimed to assess the validity of the vertical interface assumption used in current numerical models that simulate the filling of pipelines. This assessment was conducted only for horizontal slopes, for simplicity. In these experiments, the configuration with two digital camcorders was used, and it was possible to record along a 2.2 m length of the pipeline, from 10.4 m until 12.6 m from the upstream end. The camcorders were able to record 30 frames per second. The errors in the longitudinal measurement of the front feature locations was ± 0.05 m.

The goal was to record the passage of the three front features simultaneously, and represent it in charts that showed the evolution of these three features over time. This also provided an idea of the front with for each of the tested water levels at the overhead tank. The front feature locations were measured against a ruler that was placed close to the pipe.

The results of these measurements are presented in figures 4.1, 4.2 and 4.3, grouped by the relationship between the upstream pressure head H and the pipe diameter D. Each figure shows four snapshots of the front (separated by 0.1 s) plotted for each repetition. As mentioned previously, the actual shape of the front is not vertical, but instead it resembles a wedge. In general the measurements are consistent within a given value of the relation H/D among the different repetitions.

The results for H/D=9.2, the highest pressure head used in these experiments, show that in average the front length is 6.9 times the pipe diameter. The arrival time of the front feature 1 at the 11.0 m station varies between 3.8 and 4.1 seconds, and that discrepancy reflects the small differences in the flow start time among the different repetitions. Other differences in the front shape for the same repetition can be attributed to some extent to the turbulent nature of the front.

The results for H/D=6.6 are similar to the ones obtained for the case with H/D=9.2. In this case the front is slightly wider, and it spans over a length of 8.8 pipe diameters. This shows a tendency of the inflow front to become wider if the initial pressure head is smaller. The arrival time of the front feature 1 at the 11.0 m station is between 4.4 and 4.6 seconds.

The results for H/D=3.9 differ from the ones obtained for the larger pressure heads in the sense that the simultaneous recording by the camcorders could not capture the whole inflow front. In other words, the total length of the front exceeded 2.2 m, the recording width limit of the experiment. Thus, only features 1 and 2 were represented in the snapshots. Confirming the tendency of the front to be wider for smaller pressure heads, the average distance between features

1 and 2 was 10.1 times the diameter. The smaller differences between the front shapes in each snapshot reflect the less turbulent nature of the front.

Over time, it was also noticed a tendency of the fronts to increase in width as they traveled along the recording stations. Except for the 1^{st} repetition for H/D=6.6, this increase ranged between 2.0 up to 3.8 pipe diameters. This could not be measured for the cases when H/D=3.9, since the front could not be fully captured with the camcorders.

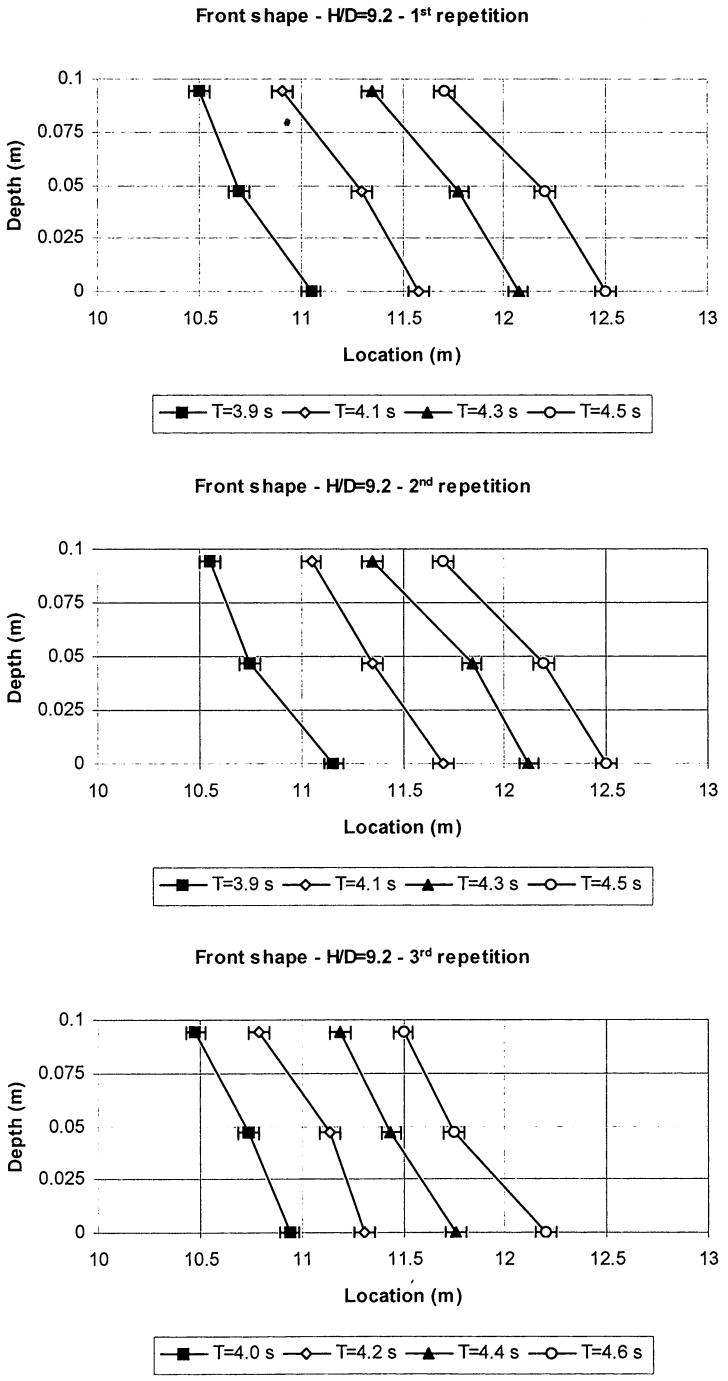

Figure 4.1: Shape of the front advance for H/D=9.2 and horizontal slope

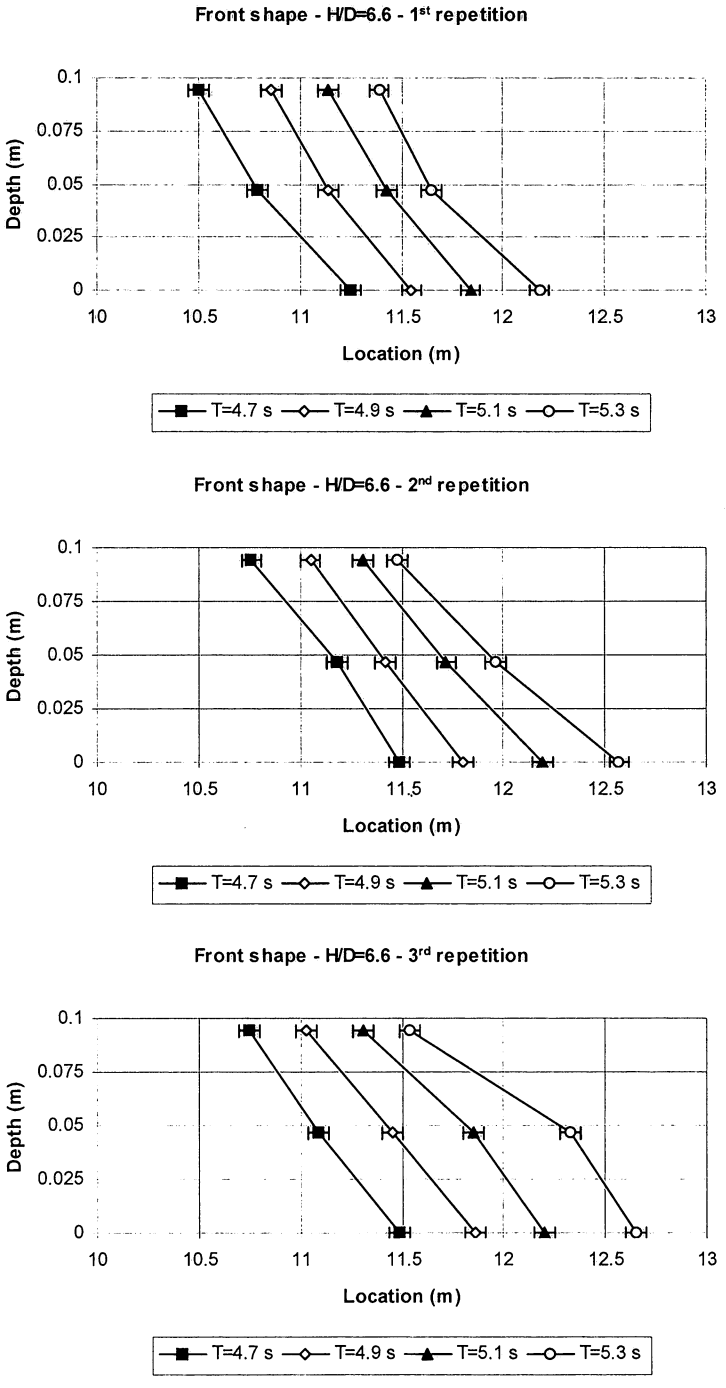

Figure 4.2: Shape of the front advance for H/D=6.6 and horizontal slope

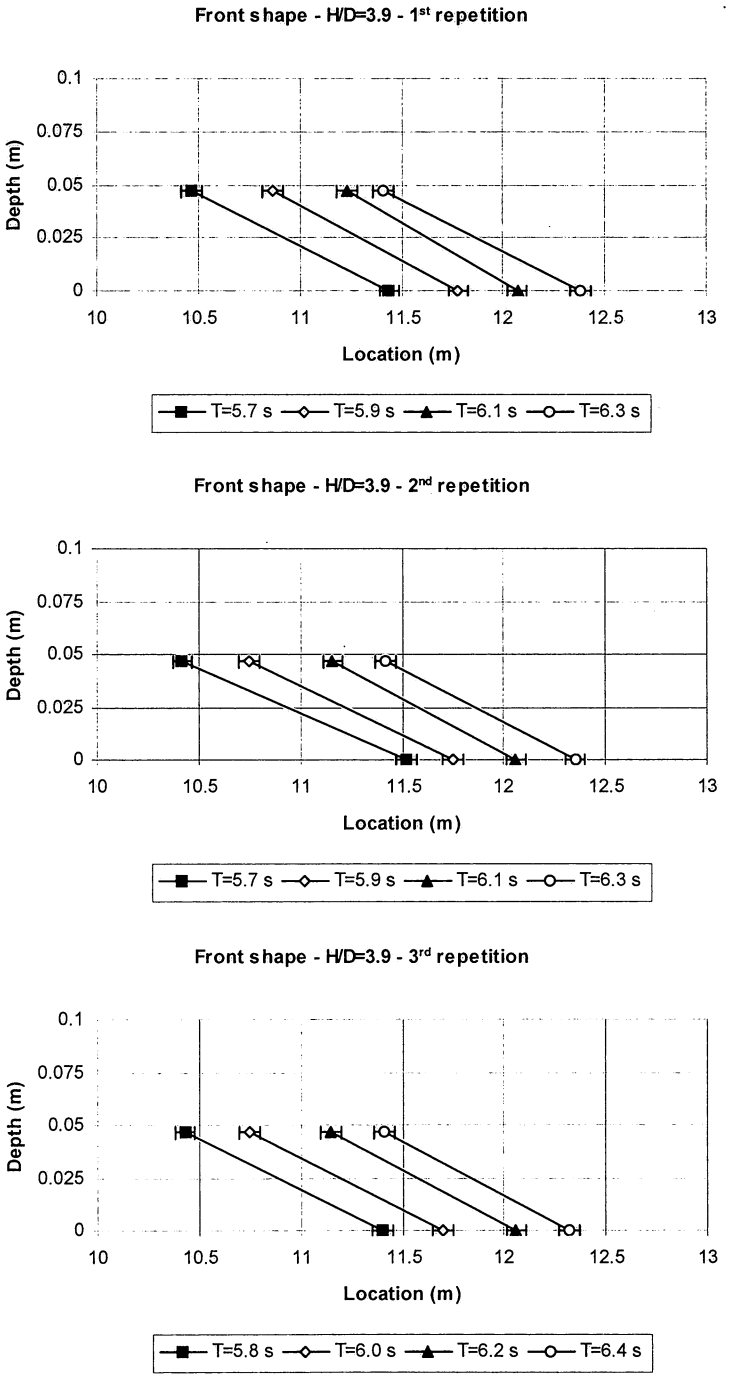

Figure 4.3: Shape of the front advance for H/D=3.9 and horizontal slope

4.2 Trajectory of front features

4.2.1 Horizontal slope

The study of the front features trajectory was conducted for each of the three slopes considered in this study. Figures 4.4, 4.5 and 4.6 present the results for the cases when the slope is horizontal and H/D=9.2, 6.6 and 3.9, respectively. Figure 4.7 presents the averaged trajectory of each front feature for the different values of H/D and horizontal slope. This average was obtained simply by calculating (for several time instants) the average location of the particular feature. The objective to calculate this average is to reduce the effect of the variability caused by the different flow start-ups between the repetitions. The average experimental error for the trajectory speed measurements was around ± 0.2 m/s for these experiments.

The results shown in figure 4.4 and averaged in figure 4.7 confirm that the fastest front speed for the horizontal slope occurred for the case where the ratio H/D was 9.2. This speed, however, is not uniform among the three different front features. The average speed of the features are 2.3 m/s, 2.2 m/s and 1.9 m/s for front features 1, 2 and 3 respectively. This shows that the two lower features have approximately the same speed, but the upper feature moves at a slower speed, which is in agreement with the previous observations which pointed to a spreading of the front. The time it takes for the front to arrive at the 11.0 m station is 4.0 seconds, and this will be used as an indicator of the average propagation speed of the front.

Figure 4.5 and the averaged trajectories shown in figure 4.7 for the case when H/D=6.6 indicate results that are similar to the previous case. The front feature speeds are generally smaller: 1.8 m/s, 1.8 m/s and 1.4 m/s for front features 1, 2 and 3 respectively. Likewise, features 1 and 2 show roughly the same speed while feature 3 moves with a smaller speed. The arrival time of the front at the 11.0 m station is 4.5 seconds.

Finally, the results for H/D=3.9 shown in figure 4.6 and averaged in figure 4.7 indicate the lowest front speeds. Front feature 1 and 2 have the same speed of 1.4 m/s. Similarly to what was presented in figure 4.3, it wasn't possible to record the passage of feature 3. As the scheme of the experimental apparatus (figure 3.1) shows, some time after the passage of the two lower features at the recording stations the front arrives at the downstream tank, causing the rise of the downstream tank water level. This increased water level generated a backward moving pipe-filling bore, that arrives at the recording location prior to the arrival of feature 3. Thus, feature 3 could not be captured for the lowest H/D case and horizontal slope. The front arrival time at the 11.0 m station is 5.4 seconds.

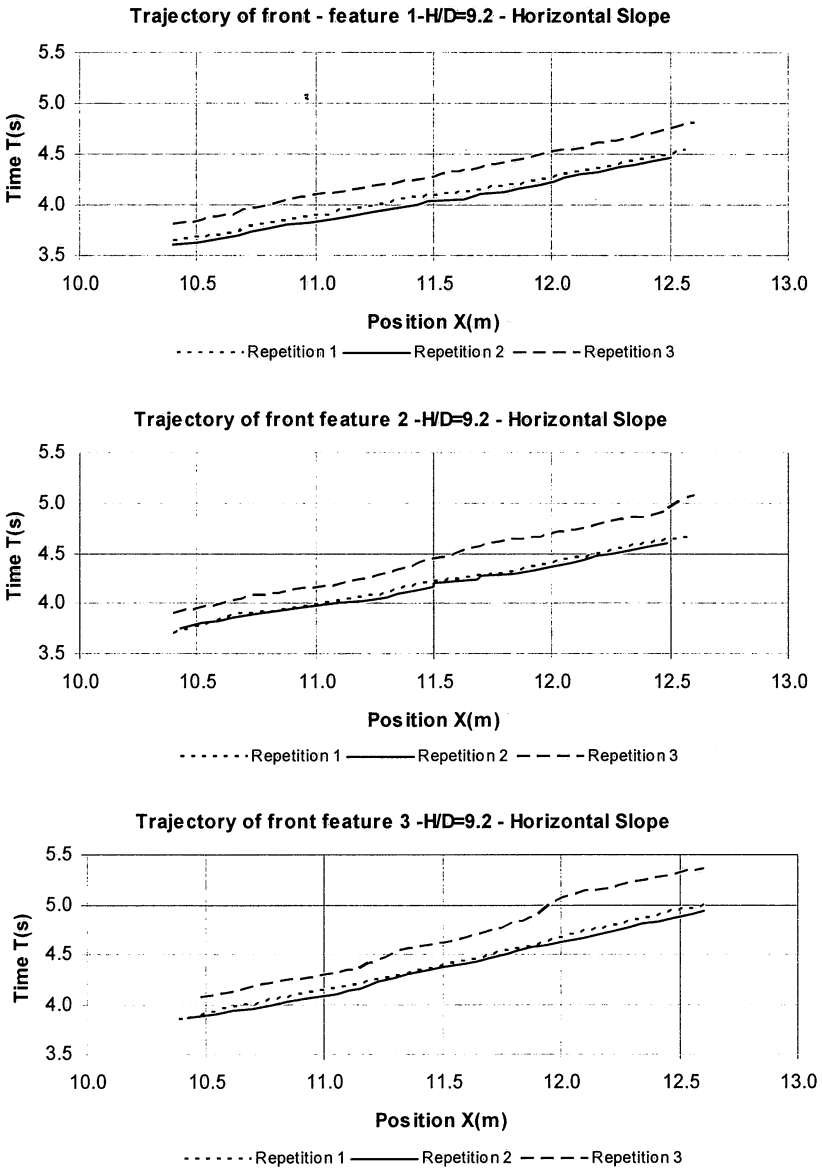

Figure 4.4: Trajectory for the three front features for H/D=9.2 and horizontal slope

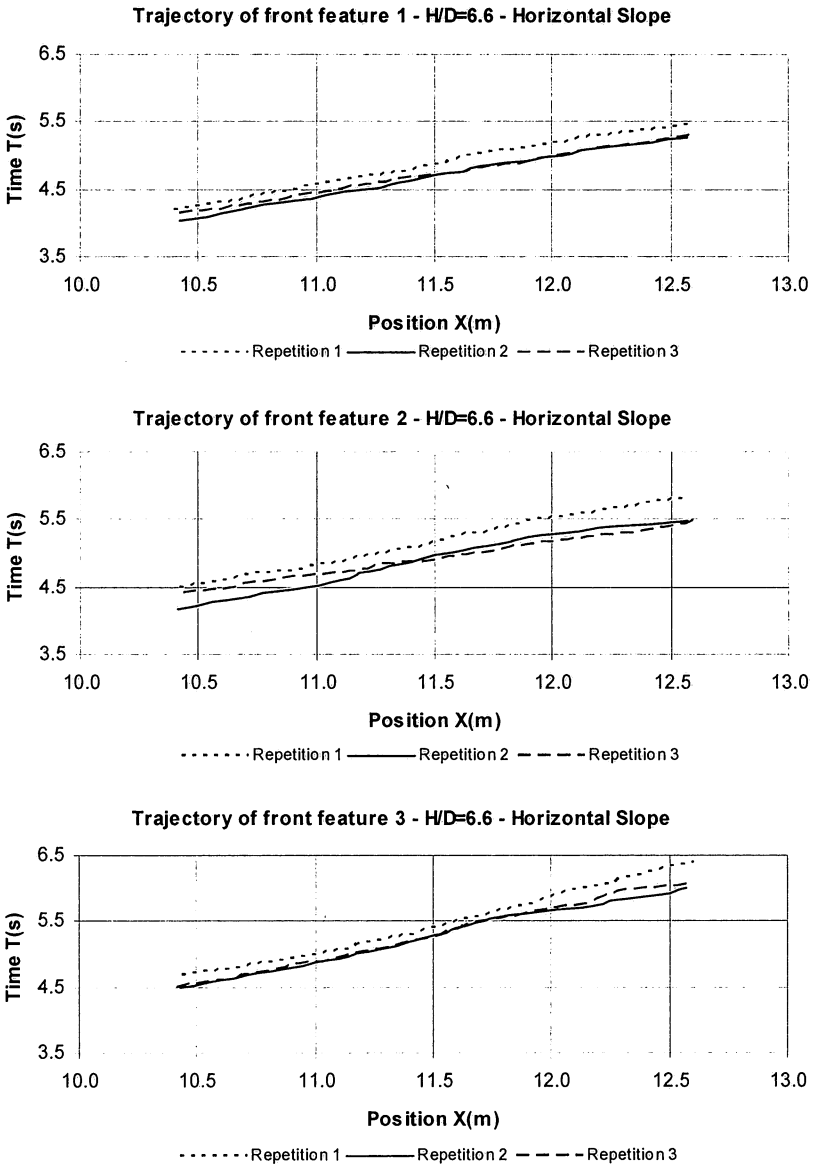

Figure 4.5: Trajectory for the three front features for H/D=6.6 and horizontal slope

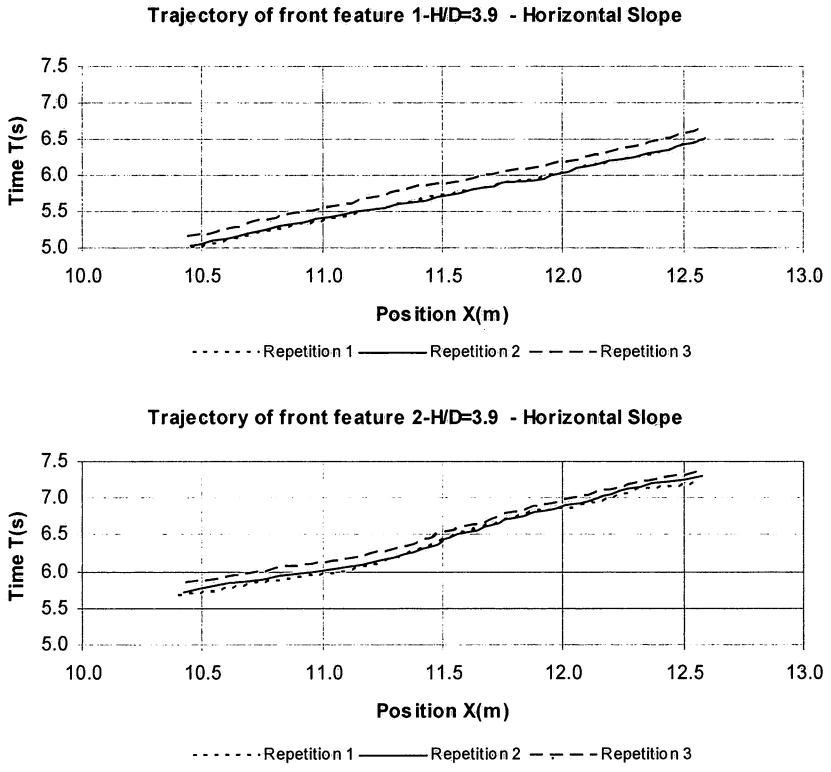

Figure 4.6: Trajectory for the three front features for H/D=3.9 and horizontal slope

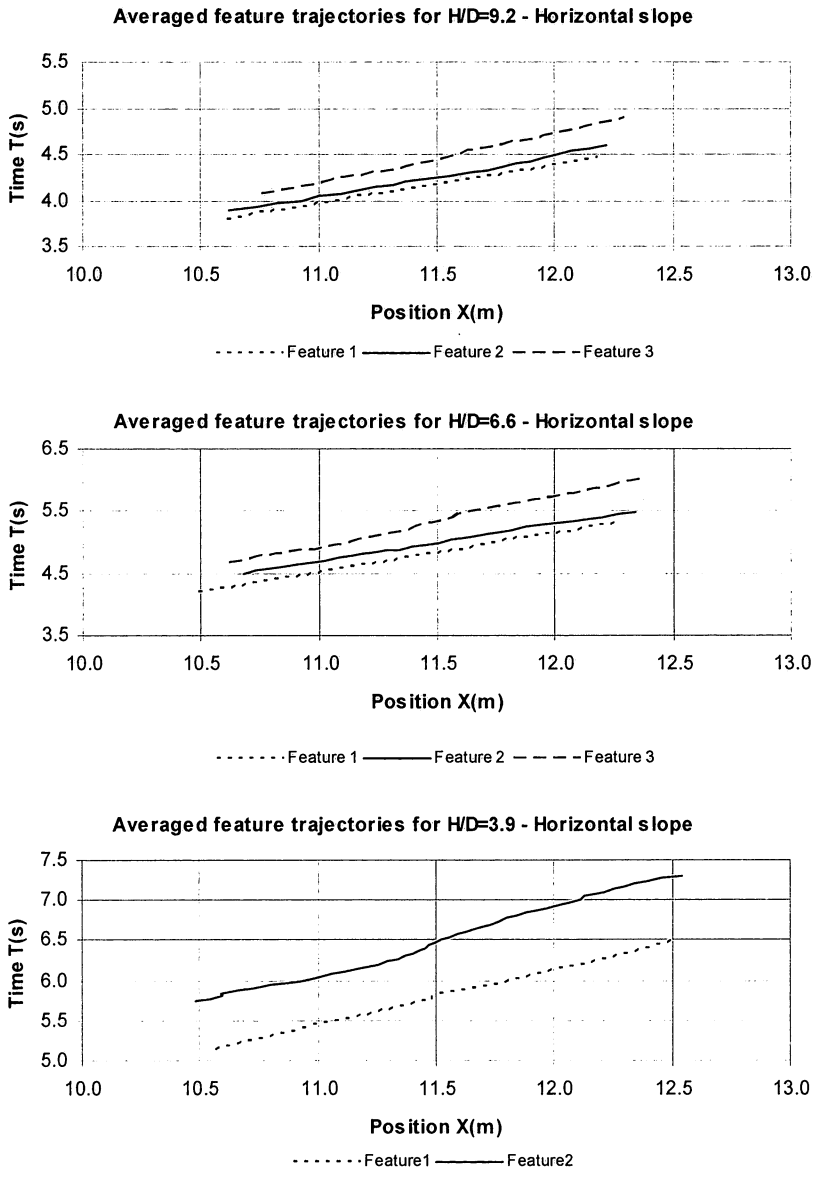

Figure 4.7: Averaged trajectory of front features for the horizontal slope

4.2.2 Upward 0.40% slope

The experiments with the upward slope were conducted after setting the flume with a 0.40% slope. A problem with one of the digital camcorders prevented the simultaneous recording of the front. As a result, separate runs were conducted in which the camcorder was either positioned in the upstream or in the downstream recording locations. After the recording, the corresponding trajectories obtained for the two stations were plotted in the same graph. This explains the reason for some discontinuities in the trajectories, albeit the experimental conditions were the same.

Although the experiments did not intend to measure the length of the front for the upward slope of 0.40%, the extrapolation of the front features' trajectories allow for an estimation of this length. These estimations suggest that the front is considerably longer, extending over 17 and 25 diameters for the case when H/D is 9.2 and 6.6 respectively. For the case when H/D=3.9, the estimated distance between features 1 and 2 is over 13 diameters.

For the case when H/D was 9.2, the speed of the front features was similar to the correspondent ones for the horizontal slope. The speeds were 2.2 m/s, 2.3 m/s and 1.9 m/s for features 1, 2 and 3 respectively. As in the previous case, features 1 and 2 have the same speed (within the experimental error), with the speed of feature 3 smaller. However, the average front speed propagation is slightly less than the horizontal case since the front feature 1 arrives at the 11.0 m station at 3.9 seconds.

For the case when H/D was 6.6, the speeds also were generally similar to the ones in horizontal slope, but some error on the trajectory propagations occurred. This is manifested in the speed of feature 2, much higher than the speed of feature 1. The data collected indicated speeds of 1.6 m/s, 2.2 m/s and 1.6 m/s for features 1, 2 and 3 respectively. The error is greater than the experimental error, and can only be attributed to a misplace in the camera location. The average front speed propagation is the same as the horizontal case, with the front feature 1 arriving at the 11.0 m station at 4.5 seconds.

Unlike the other slope results, the propagation of feature 3 could be observed for the case when H/D=3.9, but again unexpected errors have affected the front propagation speed results. In this case, the speed of feature 1 seems underestimated. The measured speeds were 1.3 m/s, 1.6 m/s and 1.5 m/s for features 1, 2 and 3 respectively, and the time required for the front to arrive at the 11.0 m station was 5.7 seconds.

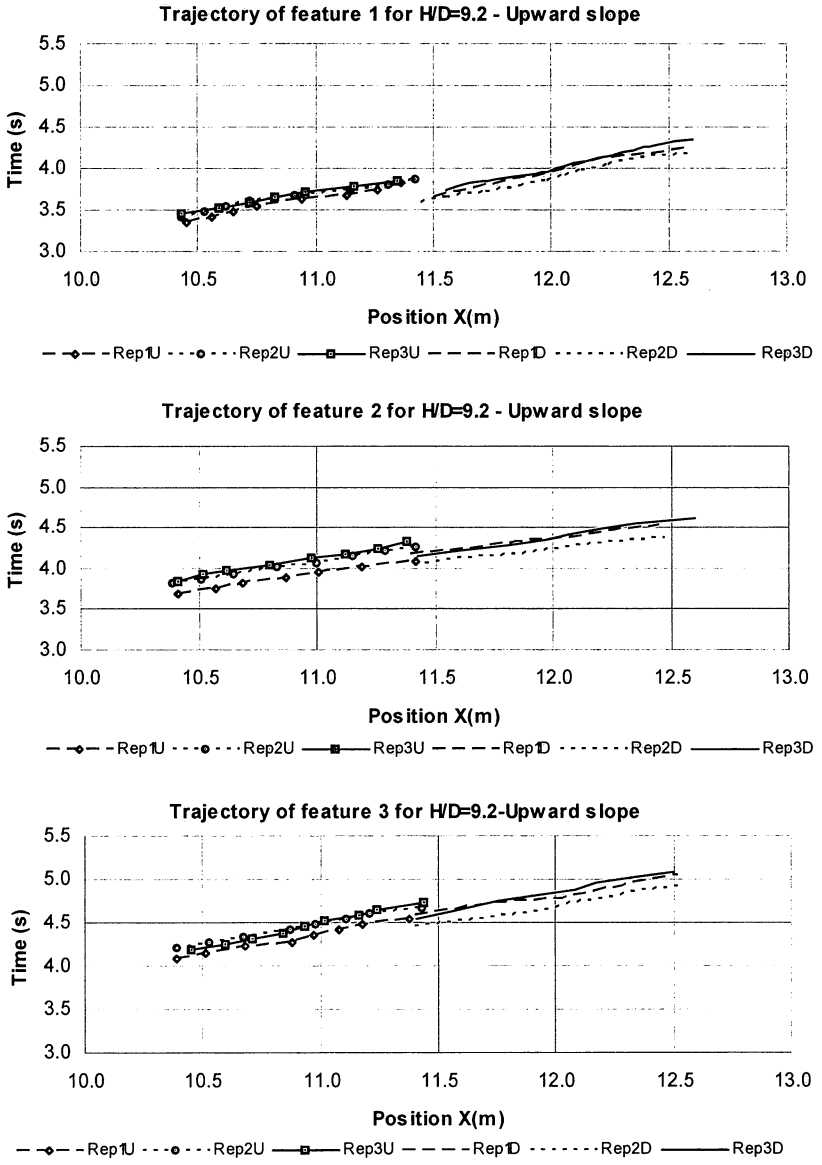

Figure 4.8: Trajectory for the three front features for H/D=9.2 and 0.40% upward slope. Rep stands for repetition, U stands for recording promoted at upstream location and D at downstream location

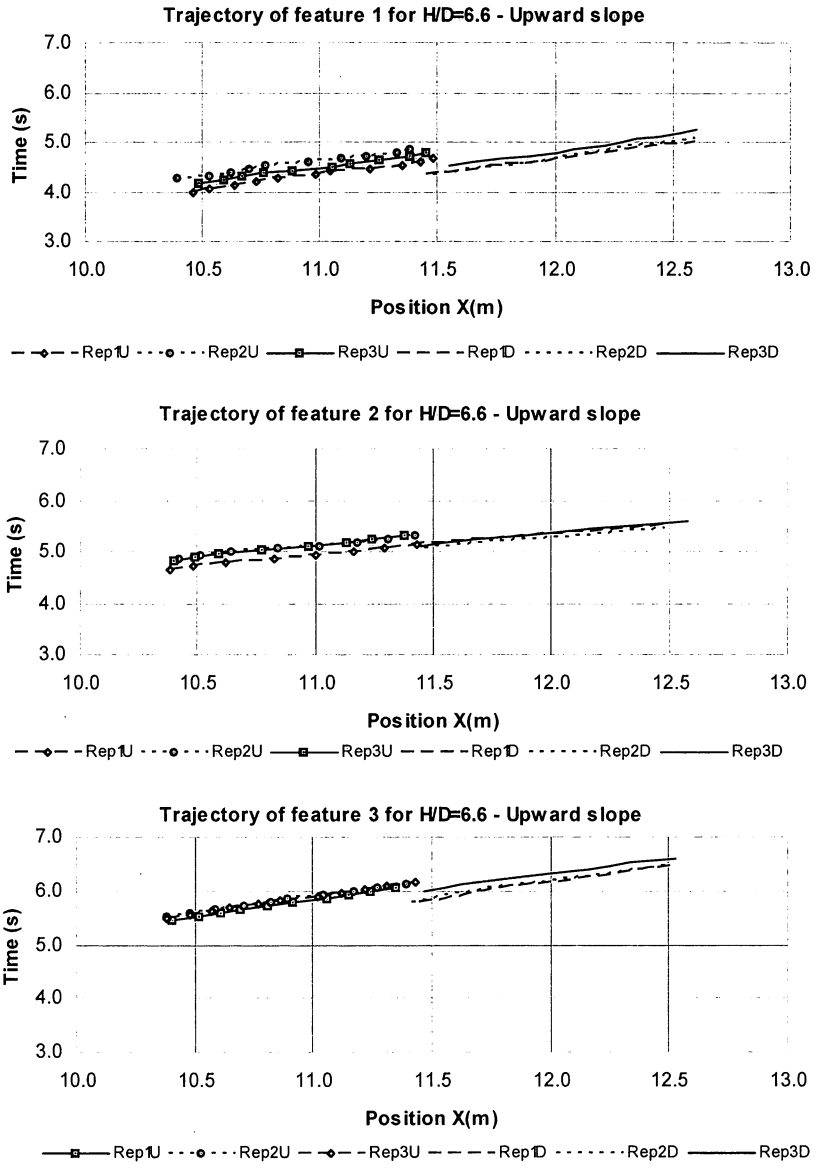

Figure 4.9: Trajectory for the three front features for H/D=6.6 and 0.40% upward slope. Rep stands for repetition, U stands for recording promoted at upstream location and D at downstream location

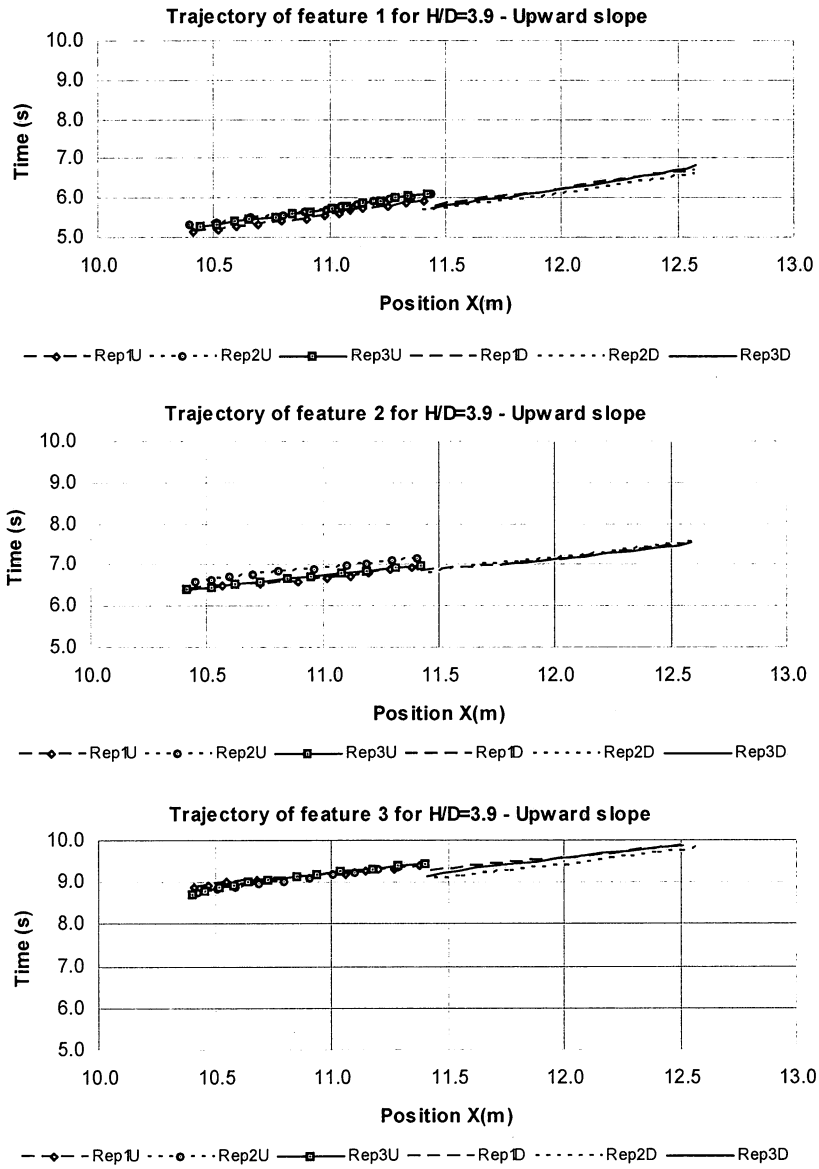

Figure 4.10: Trajectory for the three front features for H/D=3.9 and 0.40% upward slope. Rep stands for repetition, U stands for recording promoted at upstream location and D at downstream location

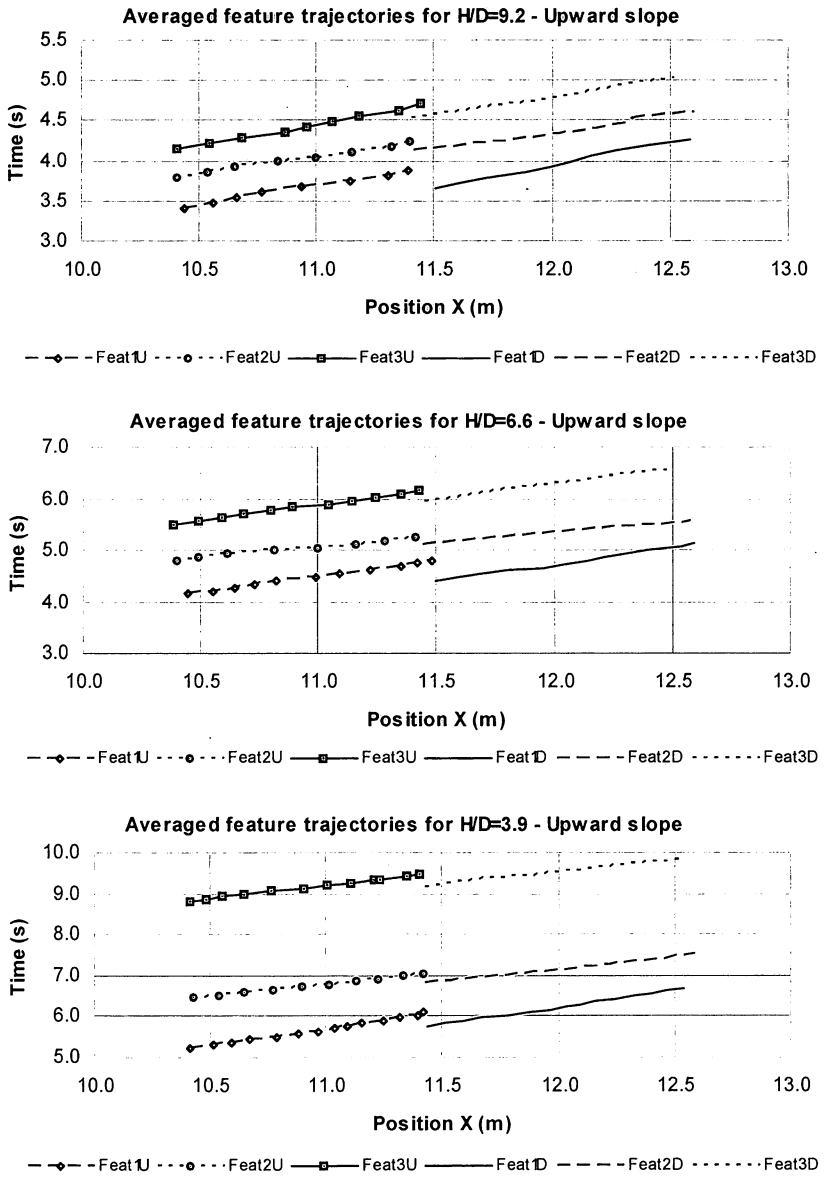

Figure 4.11: Averaged trajectory of front features for the 0.40% upward slope. Feat stands for feature, U and D are the upstream or downstream recording locations.

4.2.3 Downward 1.02% slope

Following the upward slope experiments, the flume slope was adjusted to a downward slope of 1.02%. As in the upward slope runs, these experiments were also conducted with one digital camcorder only.

As with the upward slope case, the extrapolation of the trajectories' paths allows an estimate of the length of the front. This estimation leads to longer fronts if compared to the horizontal slope case. The front lengths (normalized by the pipe diameter) were over 13 and 17 for the H/D=9.2 and 6.6 cases, respectively. The distance between features 1 and 2 for the case when H/D is 3.9 was over 13 times the diameter. The fronts advances generally 10% faster than the correspondent cases for the horizontal slope.

For the case when H/D was 9.2, the speed of the front features was very similar to the correspondent case for the horizontal slope, expect for feature 3, which had a smaller speed. The speeds were 2.3 m/s, 2.2 m/s and 1.5 m/s for features 1, 2 and 3 respectively. This again shows the tendency of the front to spread as it moves downstream. However, the average front speed propagation is faster than the horizontal case since the front feature 1 arrives at the 11.0 m station at 3.6 seconds. The trajectory plots also suggest some type of systematic error for the feature 3 when the camera was positioned at the upstream recording station.

For the case when H/D was 6.6, the speeds were smaller than the previous case, but comparable to the speed observed for the horizontal slope case. The speeds were 1.8 m/s, 1.7 m/s and 1.5 m/s for features 1, 2 and 3 respectively, showing the front spreading tendency. The average front speed propagation is faster than the horizontal case, with the front feature 1 arriving at the 11.0 m station at 4.0 seconds.

Finally, for the smaller H/D of 3.9 the front speed was measured for the two lower front features 1 and 2. The speeds were slightly higher than the case for the horizontal slope, with both features moving at 1.6 m/s speed. As with the previous cases, the average front speed propagation is faster than the horizontal case, with the front feature 1 arriving at the 11.0 m station at 5.0 seconds.

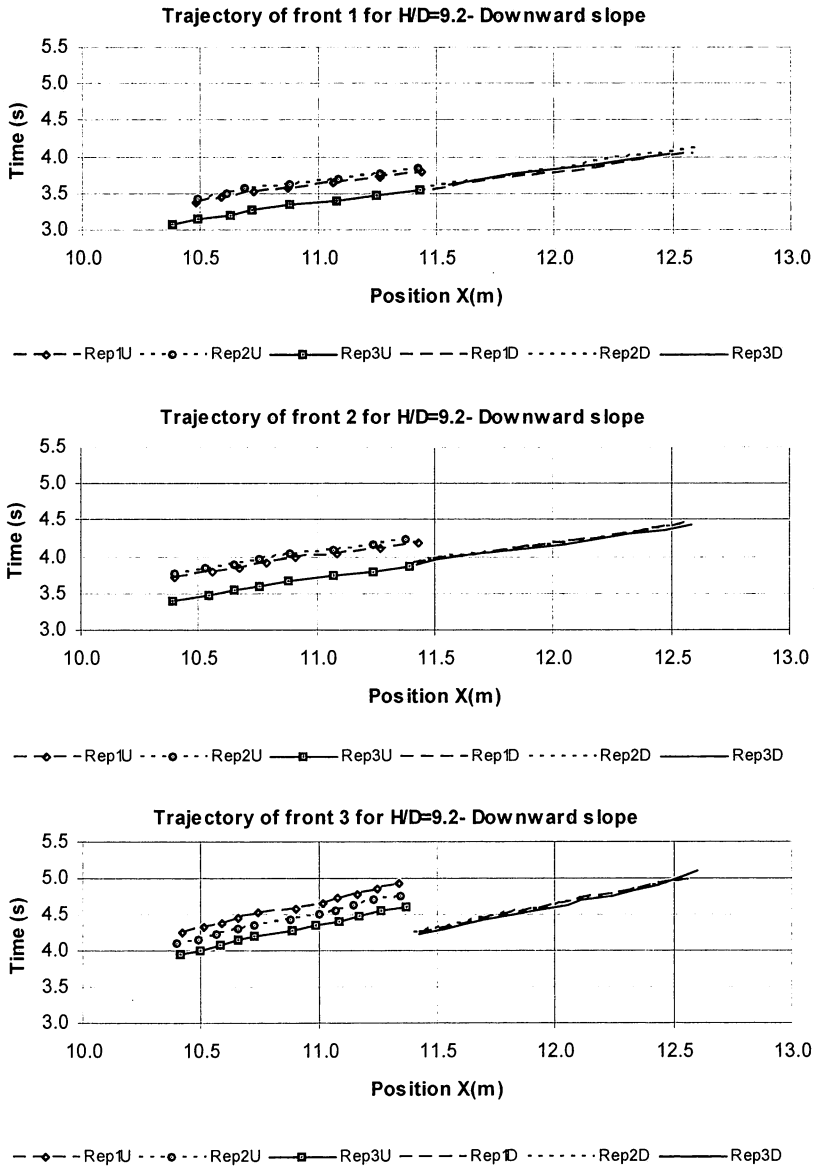

Figure 4.12: Trajectory for the three front features for H/D=9.2 and 1.02% downward slope. Rep stands for repetition, U stands for recording promoted at upstream location and D at downstream location

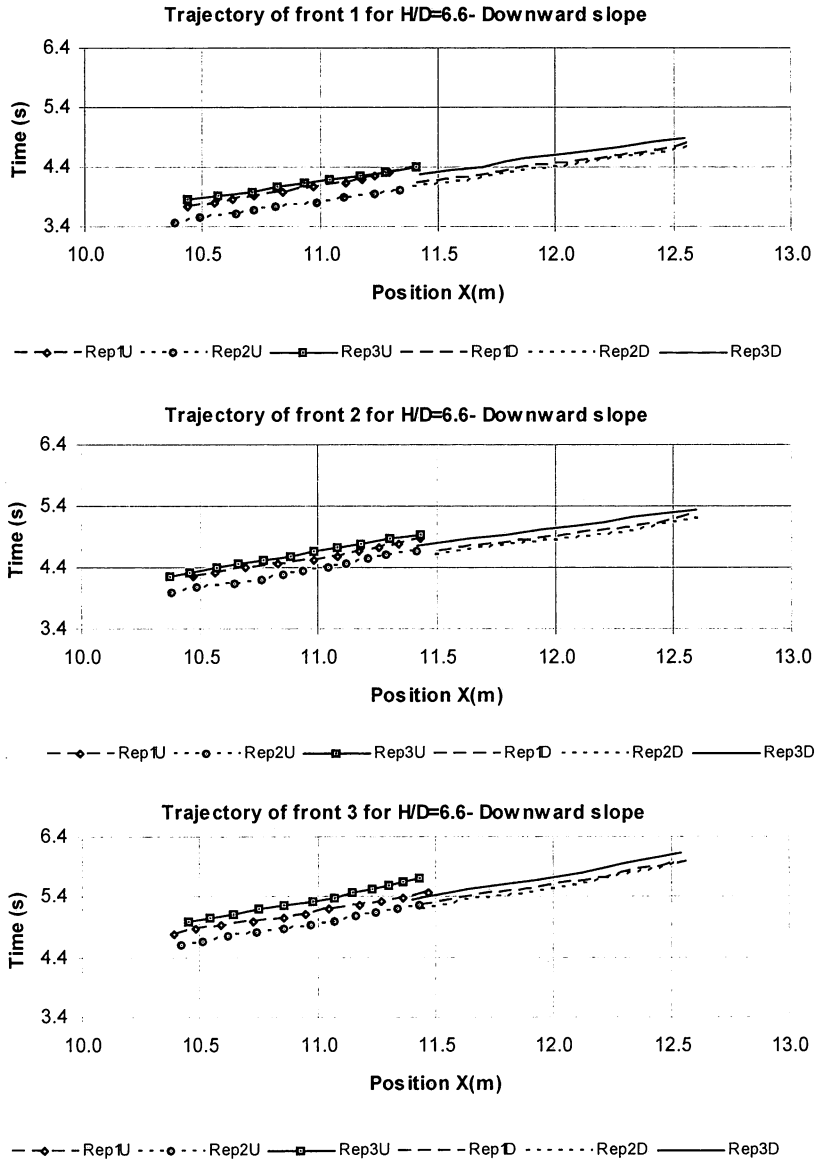

Figure 4.13: Trajectory for the three front features for H/D=6.6 and 1.02% downward slope. Rep stands for repetition, U stands for recording promoted at upstream location and D at downstream location

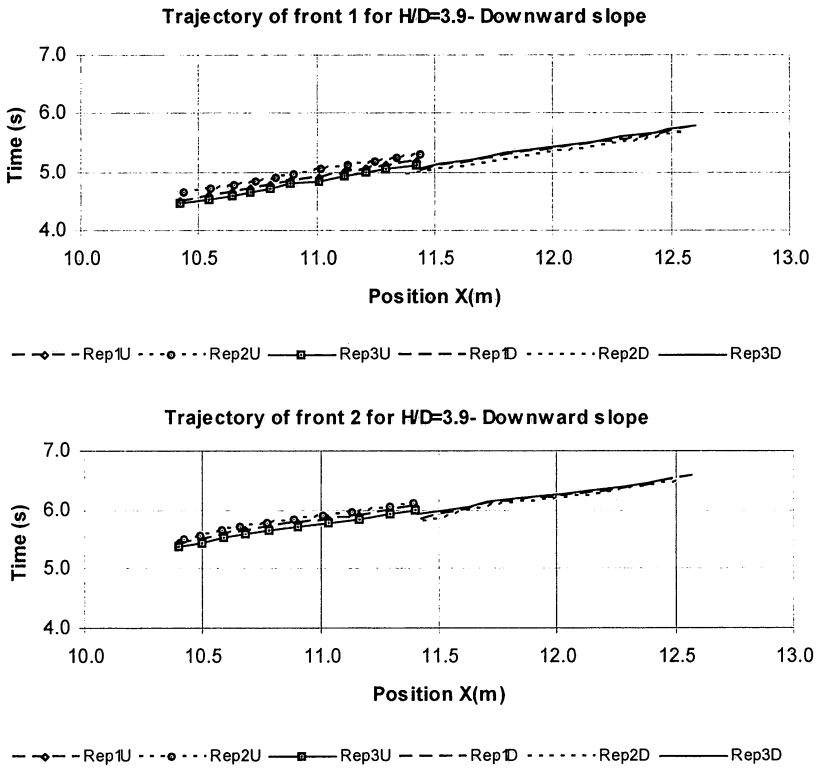

Figure 4.14: Trajectory for the three front features for H/D=3.9 and 1.02% downward slope. Rep stands for repetition, U stands for recording promoted at upstream location and D at downstream location

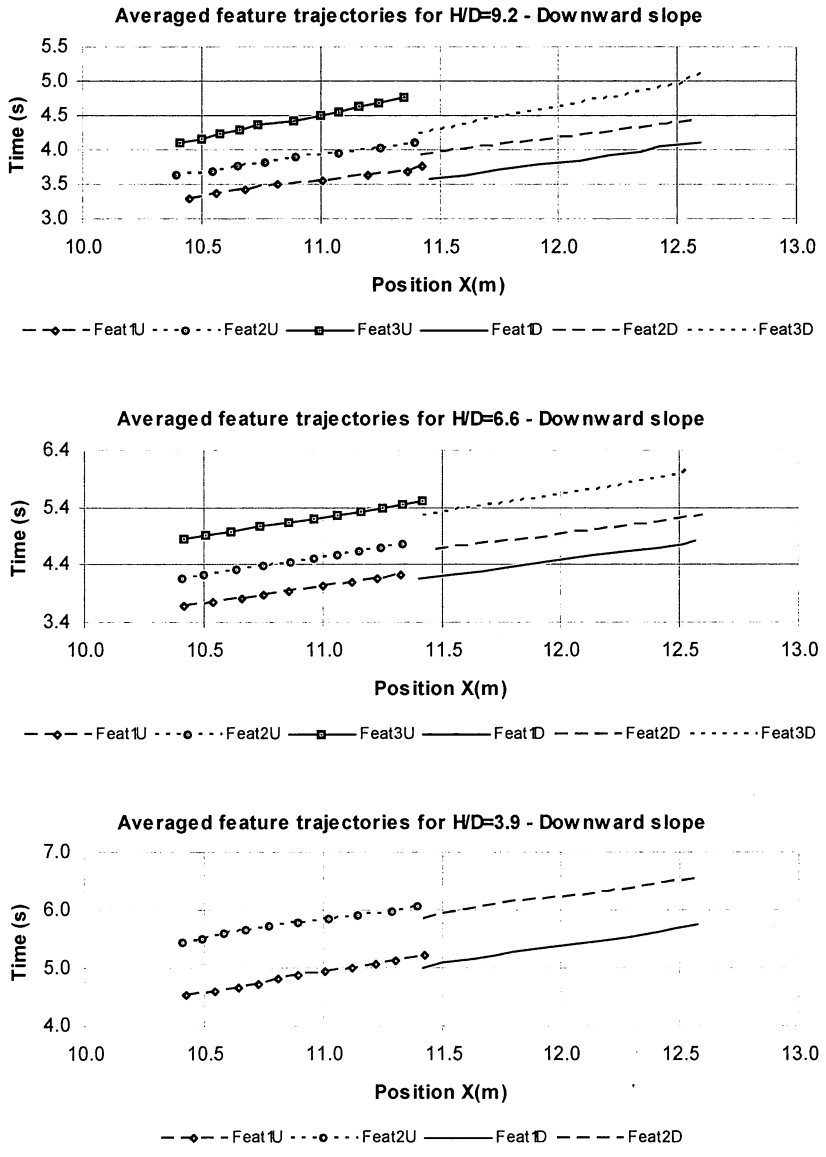

Figure 4.15: Averaged trajectory of front features for the 1.02% downward slope. Feat stands for feature, U and D are the upstream or downstream recording locations.

4.3 Pressure measurements of the inflow front

This section presents the results from the measurements made with the piezo-resistive pressure transducer located at the bottom of the pipe at the 12.6 m station. The pressure head results are also compared with the depth changes observed at the same station recorded with the digital camera.

The calibration of the transducer was promoted at each experimental run. The transducer was started with the empty pipeline. Some time after the start, the inflow front passed the transducer location, and eventually reached the downstream tank. The water level raised at that tank, and soon after the overflow occurred at that tank the inflow was stopped at the upstream end. The recording with the transducer lasted for 100 seconds, when residual oscillations at the downstream tank eventually were minimal. The final water level at the tank (measured from the pipe bottom) was used to promote the transducer calibration for the particular run.

In general, the results obtained with the transducers are characterized by a sharp increase followed by a less steep increase in the pressure head. The three repetitions for each case studied tend to agree well, and existing discrepancies between runs may be related to problems in the pressure transducer calibration for that particular run or for differences in the start-up of the upstream valve.

The depth changes observed in the movies and the pressure transducer are generally in good agreement. There is a tendency of the measured pressure head to have a sharper rise than the depth recorded in the movies. This could possibly be due to vertical acceleration of the fluid at the vicinity of the front. However, this can only be confirmed by further experiments in which the velocity components at the front would be measured. Because such velocity measurements would need to be taken in a relatively thin layer within a closed pipe some technical difficulties could arise. An alternative for these measurements could be the use of PIV instrumentation.

Finally, it is interesting to notice the pressure oscillations observed when H/D=3.9 caused by the air bubble expulsion at the downstream tank. These oscillations are significant, and one assumes that they could also occur in actual systems when air bubbles are expelled at venting points initially filled with water. It is also noticeable that the worst agreement between the camera and transducer data occurred for the downward slope case. One speculates that this could be caused by the faster moving front and more prominent non-hydrostatic conditions.

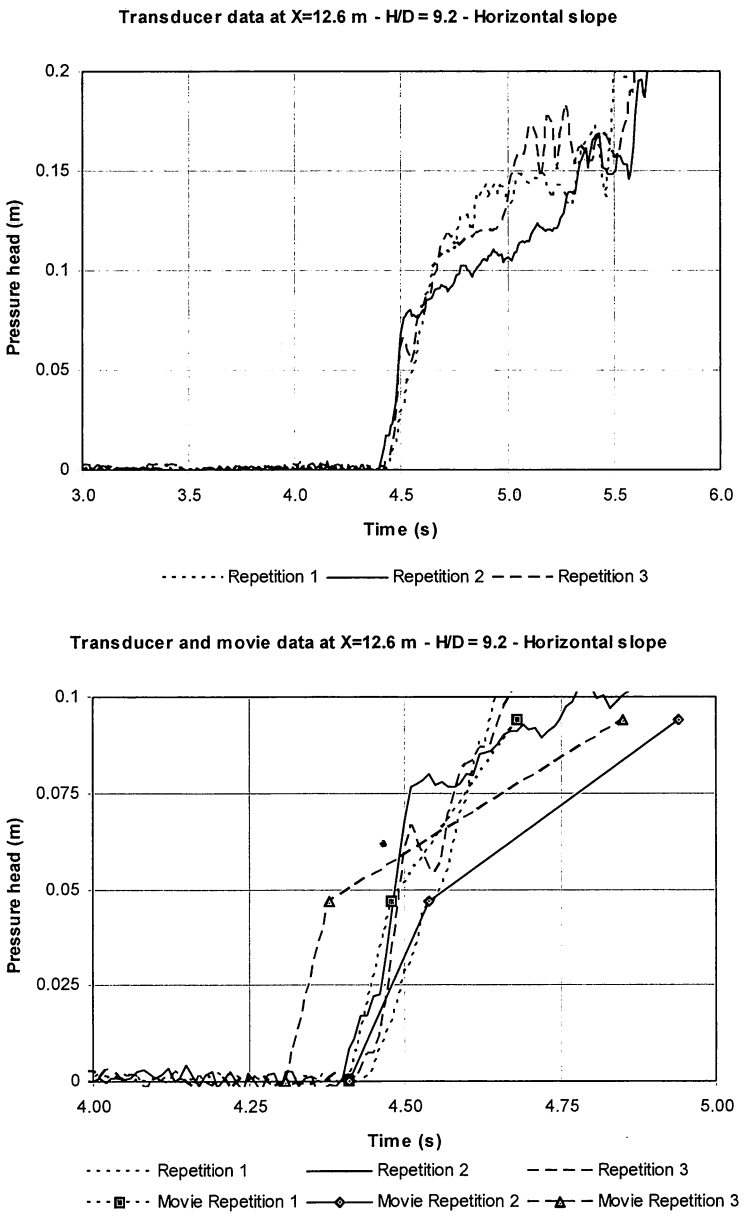

Figure 4.16: Pressure head measurements obtained with the transducer at the 12.6 m station for H/D=9.2 and horizontal slope. Lower plot show the comparison with the movie depth results.

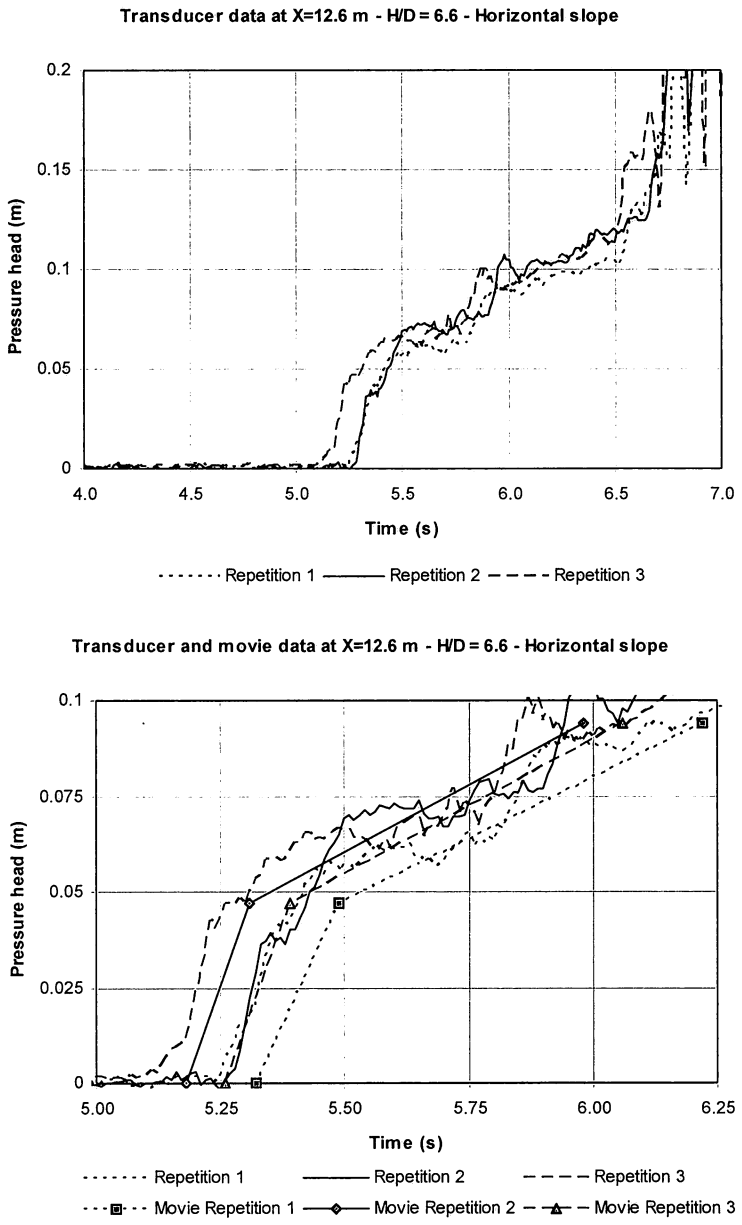

Figure 4.17: Pressure head measurements obtained with the transducer at the 12.6 m station for H/D=6.6 and horizontal slope. Lower plot show the comparison with the movie depth results.

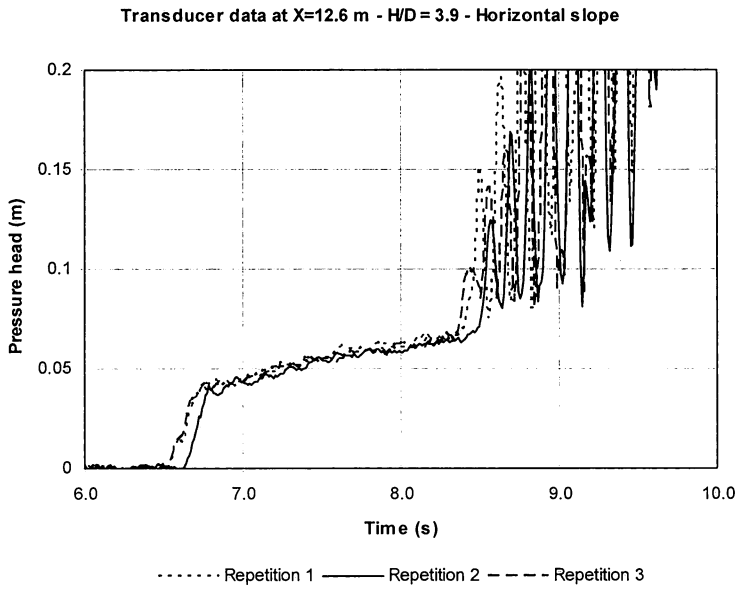

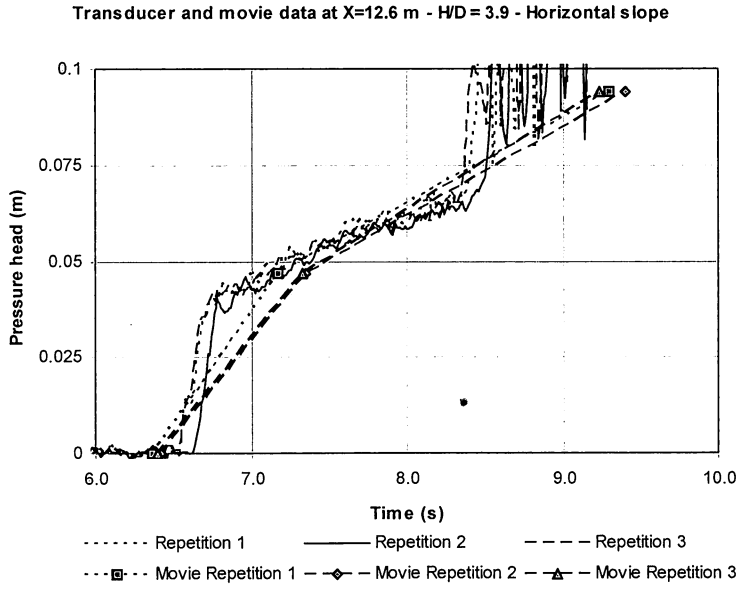

Figure 4.18: Pressure head measurements obtained with the transducer at the 12.6 m station for H/D=3.9 and horizontal slope. Lower plot show the comparison with the movie depth results. The pressure oscillations after 8 seconds reflect the front arrival at the downstream box and air bubbles being expelled at that location.

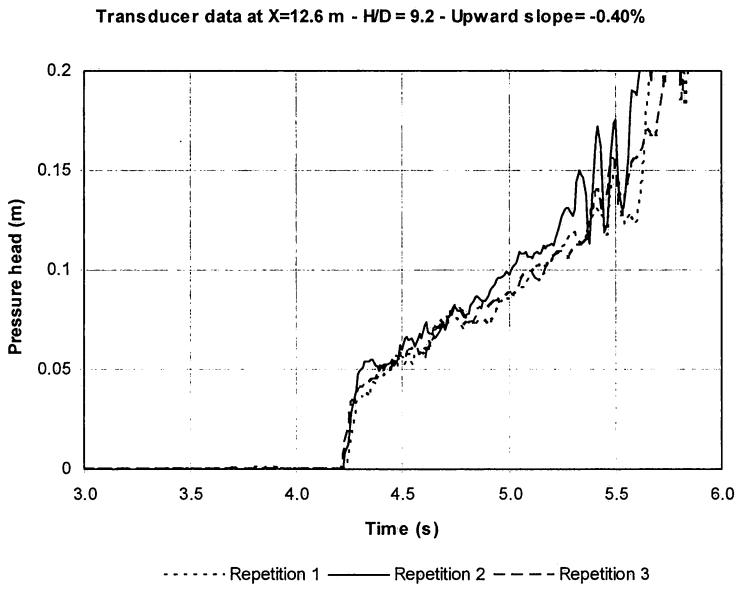

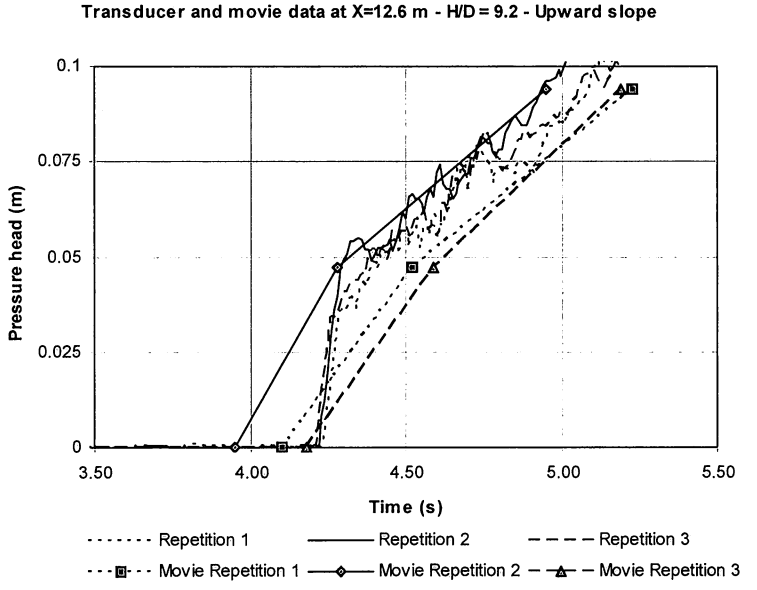

Figure 4.19: Pressure head measurements obtained with the transducer at the 12.6 m station for H/D=9.2 and 0.40% upward slope. Lower plot show the comparison with the movie depth results.

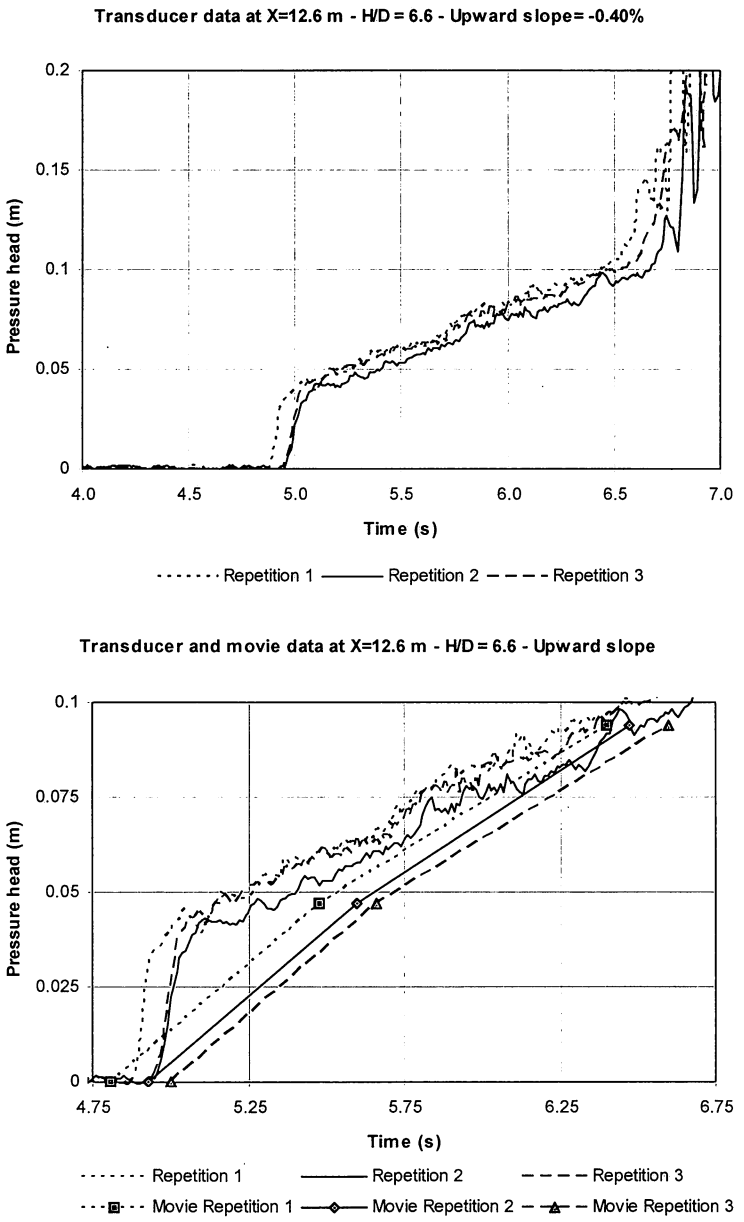

Figure 4.20: Pressure head measurements obtained with the transducer at the 12.6 m station for H/D=6.6 and 0.40% upward slope. Lower plot show the comparison with the movie depth results.

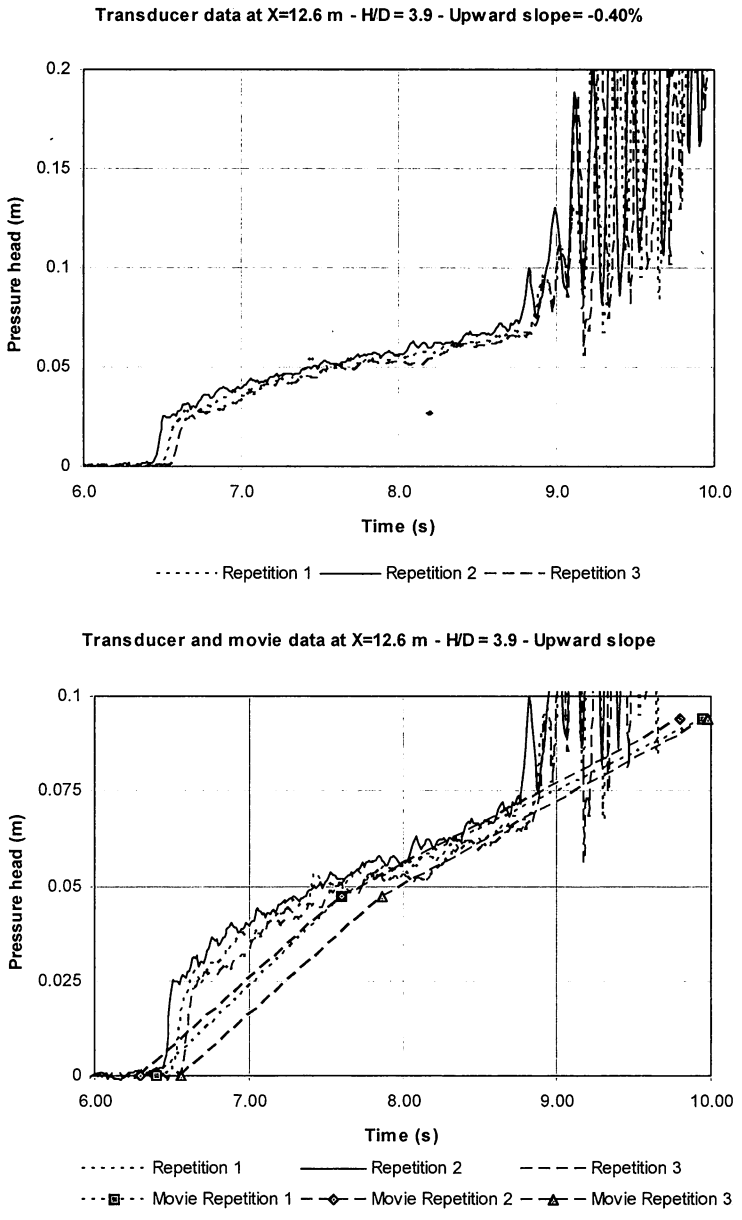

Figure 4.21: Pressure head measurements obtained with the transducer at the 12.6 m station for H/D=3.9 and 0.40% upward slope. Lower plot show the comparison with the movie depth results. The pressure oscillations after 8 seconds reflect the front arrival at the downstream box and air bubbles being expelled at that location.

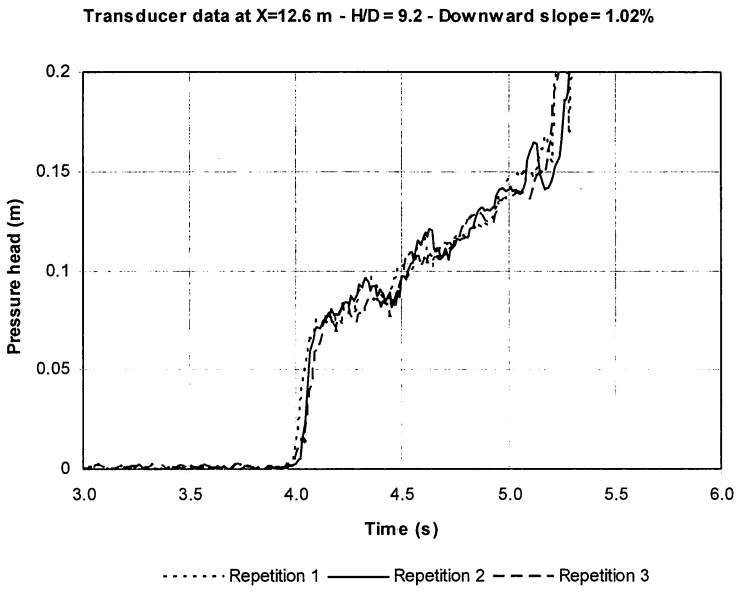

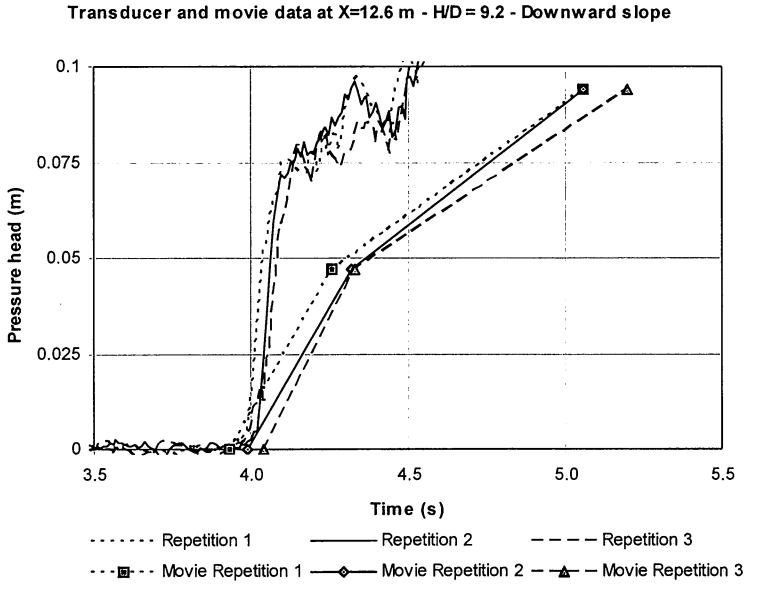

Figure 4.22: Pressure head measurements obtained with the transducer at the 12.6 m station for H/D=9.2 and 1.02% downward slope. Lower plot show the comparison with the movie depth results.

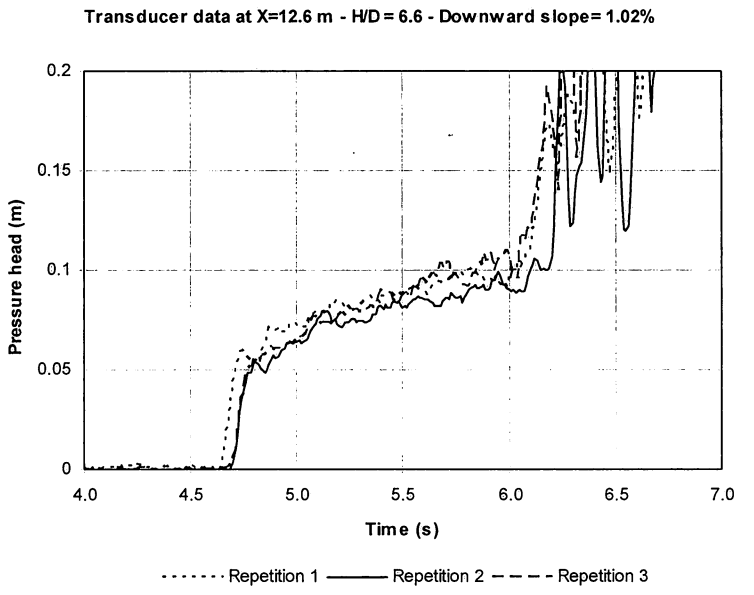

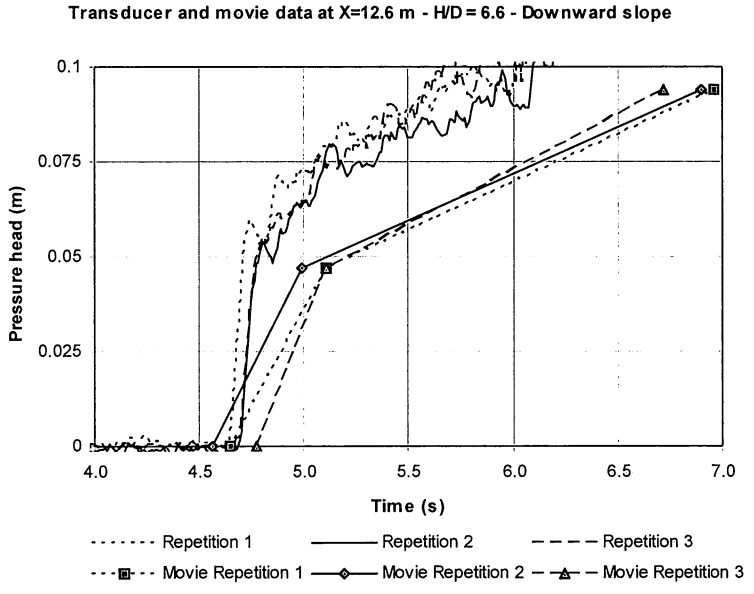

Figure 4.23: Pressure head measurements obtained with the transducer at the 12.6 m station for H/D=6.6 and 1.02% downward slope. Lower plot show the comparison with the movie depth results.

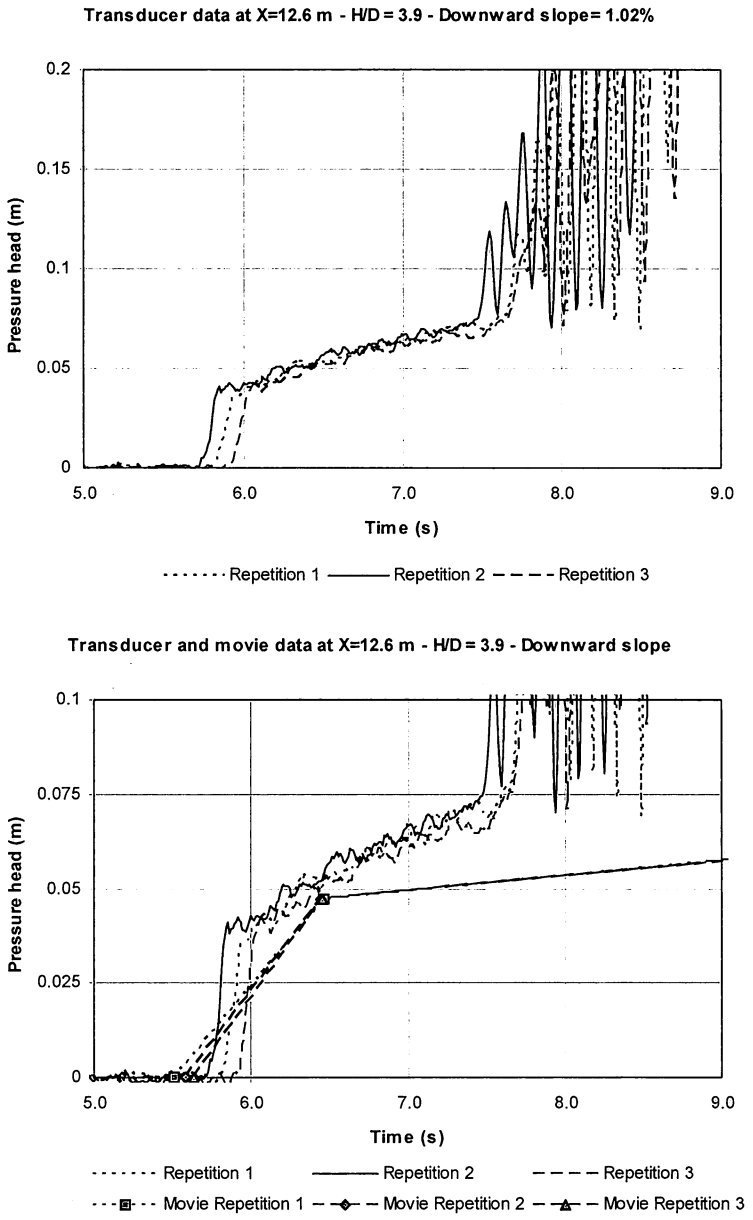

Figure 4.24: Pressure head measurements obtained with the transducer at the 12.6 m station for H/D=3.9 and 1.02% downward slope. Lower plot show the comparison with the movie depth results. The pressure oscillations after 8 seconds reflect the front arrival at the downstream box and air bubbles being expelled at that location.

4.4 Numerical predictions

This section of the report contains a comparison between the experimental data and two different numerical models to simulate the rapid filling process in the pipes. The first model approach is based on a rigid column assumption (lumped inertia analysis) and requires the assumption of a vertical interface for the advancing water front. The second method is based on the solution of the Saint-Venant equations modified to account for the possibility of the flow regime transition. While this method does calculate the shape of the free surface (no vertical interface assumption requirement), it assumes that the shallow water equations are valid, thus neglecting vertical acceleration terms. The model approach that is chosen in this study to solve the Saint-Venant equation is based on the Decoupled Pressure Approach (Vasconcelos et al., 2005).

4.4.1 Rigid column model

Examples of models based on the rigid column assumption to simulate the filling of the pipeline are provided by Liou and Hunt (1996); Izquierdo et al. (1999). Briefly, the models start with an estimated length of the pressurized water column in the pipeline. Then a momentum balance is formulated for this column in which the velocity of the column is updated at each time step. The forces considered in the momentum balance are the upstream pressure force from the supply reservoir, frictional forces and gravitational forces in cases when the pipe is sloped. Considering the local losses at the exit of the upstream reservoir with head H_R and neglecting the local acceleration terms at the reservoir exit during to the flow start-up, one can derive the following ordinary differential equation representing the momentum balance:

$$\frac{dV}{dt} = \frac{g}{L}\left(H_R - K\frac{V^2}{2g}\right) + g\sin\theta - \frac{fV^2}{2D} \tag{4.1}$$

In the above equations V is the rigid column speed, g is the gravity acceleration, L is the length of the pressurized column, H_R is the head at the reservoir, K is the localized loss coefficient at the reservoir outlet, θ is the pipeline angle with the horizontal, f is the Darcy-Weisbach friction factor and D is the pipeline diameter. The calculation procedure of this ODE was conducted with a Runge-Kutta 4^{th} order procedure (Press et al., 1989). An initial estimation of the pressurized column was required, taken here to be 10% of D. The time step was taken according to the suggestion by Zhou et al. (2002) for a similar problem:

$$dT = 0.001L\sqrt{\frac{1 - L_{init}/L_{pipe}}{gH_{atm}}} \tag{4.2}$$

In which: L_{init} is the initial estimated length of the pressurized column, L_{pipe} is the total length of the pipeline, and H_{atm} is the atmospheric pressure head (10.3 m at sea level).

The comparison between the pressure head at the 12.6 m station between the rigid column model and the experiments is shown in figure 4.25. The pressures were calculated accounting the energy losses from the upstream reservoir up to the 12.6 m station. It is at first surprising to notice that the predicted pressure heads are negative (below the pipe cross section) at the vicinity of the front. However, the fact that this approach predicts a decrease in the velocity of the advancing front is coherent with the occurrence of negative pressure heads prior to the front location, or else the front would continue to accelerate as it advanced through the pipe.

Also it is noticed that the predicted arrival of the front (signaled by the change in the pressure head from zero) occurs earlier than expected. This is better visualized in figure 4.26 where the trajectories for the three H/D values and the horizontal slope are plotted.

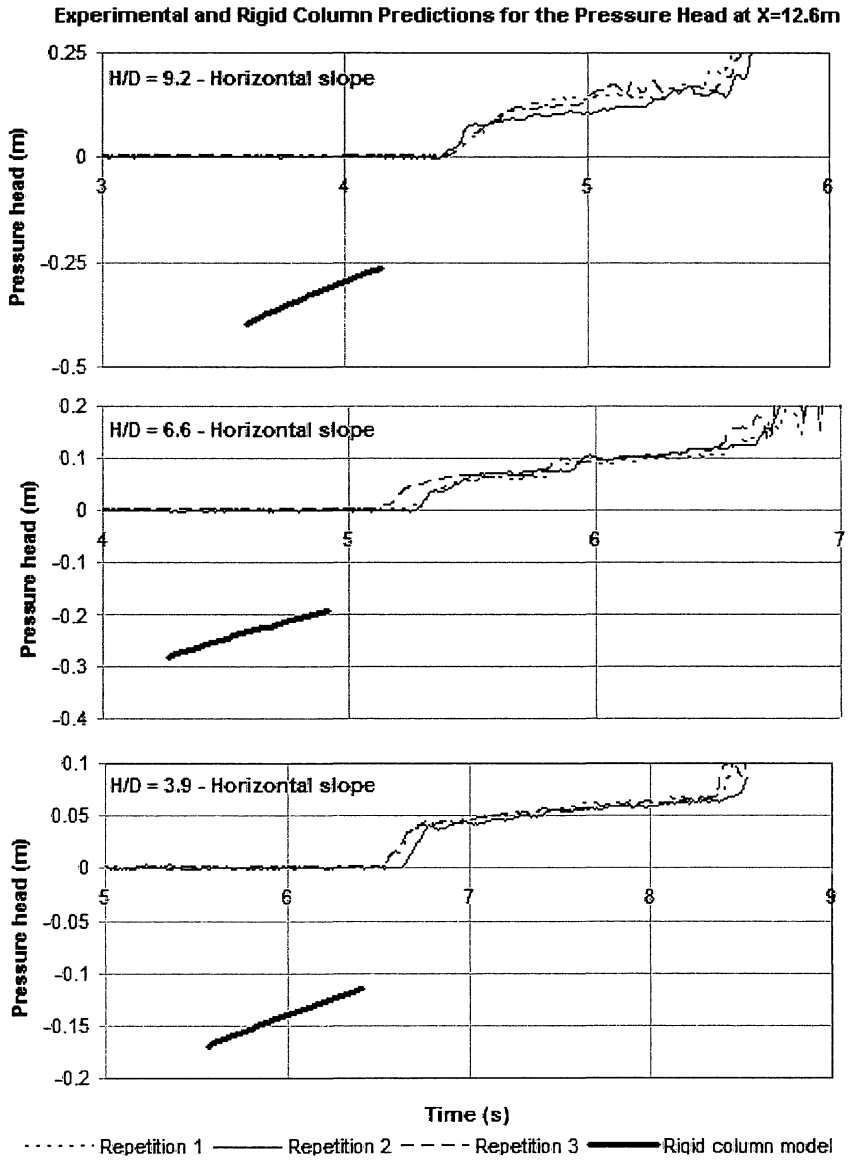

Figure 4.25: Pressure head measurements obtained with the transducer at the 12.6 m station for horizontal slope and numerical predictions from the Rigid column model.

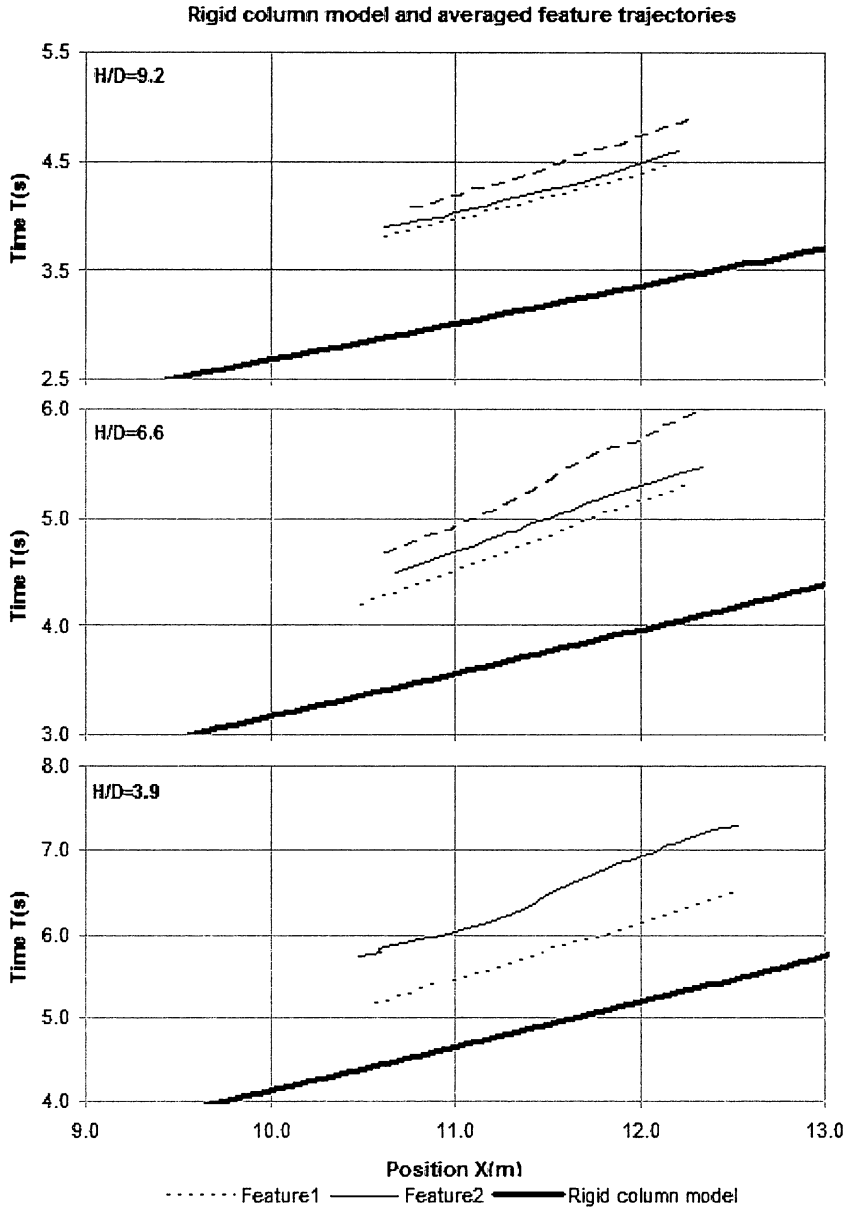

Figure 4.26: Comparison between the experimental measurement of the flow front trajectories and the front prediction from the rigid column model.

4.4.2 DPA model

The Decoupled Pressure Approach (DPA) was proposed by Vasconcelos et al. (2005) with the objective to simulate flow regime transition events in closed pipes. This method is suitable to describe the filling process in the pipeline since both free surface and pressurized conditions are likely to co-exist. It is not the objective to discuss the method here, only the equations used are presented.

For prismatic channels, without lateral inflow or outflow, the modified Saint-Venant equations, expressed in a vectorial,conservative form are given by:

$$\frac{\partial \vec{U}}{\partial t} + \frac{\partial \vec{F}}{\partial x} = \vec{S} \tag{4.3a}$$

$$\vec{U} = \begin{bmatrix} A \\ Q \end{bmatrix}, \vec{F} = \begin{bmatrix} Q \\ \frac{Q^2}{A} + gA(h_c + h_s) \end{bmatrix} \tag{4.3b}$$

$$\vec{S} = \begin{bmatrix} 0 \\ gA(S_o - S_f) \end{bmatrix} \tag{4.3c}$$

In the above equations, A is cross sectional area of water flow, Q is the water flow rate, h_c the depth of the centroid of the cross sectional area, S_o is the bed slope and S_f is the energy slope (given by the Manning equation in this implementation with n=0.010). The modification implemented by the DPA approach is related to the calculation of the surcharge pressure head h_s. This term vanishes for free-surface flows, but if the flow is pressurized, h_s can be calculated in terms of the surcharge area,defined as the difference between the flow area and the pipe area, ΔA:

$$h_s = \frac{a^2}{g} \frac{\Delta A}{A_{pipe}} \tag{4.4}$$

In which a is the acoustic wavespeed on the pressurized portion of the flow. Equation 4.4 is constructed on the assumption of flexible pipes (Wylie and Streeter, 1993), a required assumption of the DPA model. This model, while it is relatively new, has been successfully tested against experimental data and compared very well with other transient flow solvers. Different numerical schemes can be used to solve equation 4.3c, and in this study the approximate Riemann solver proposed by Roe (1981) was chosen.

The results from the pressure predictions from the DPA model at the 12.6 m station are plotted against the experimental measurements in figure 4.27. One can immediately notice that the results are much closer than the correspondent ones from rigid column model. The arrival time of the front is almost the same as the experiments for all cases considered, with the largest discrepancy occurring for the H/D=9.2. There's also a tendency of the predicted pressures to be smaller than the measured values, particularly for larger H/D. The speculation is that this is related to the fact that the shallow water equations neglect the vertical accelerations, which could be an important factor in the particular case.

The results for the predicted trajectories are shown in figure 4.28. Unlike the rigid column model, because the shape of the free surface is calculated, it is possible to distinguish the three flow features in the problem. In general, the trajectory for both of the two lower features is well predicted, while the predicted feature 3 is well behind the observed one. This indicates a greater

diffusion of the predicted pressurization front. Again, one anticipates that a better treatment for the advancing front that consider the localized vertical accelerations at the front could improve the results.

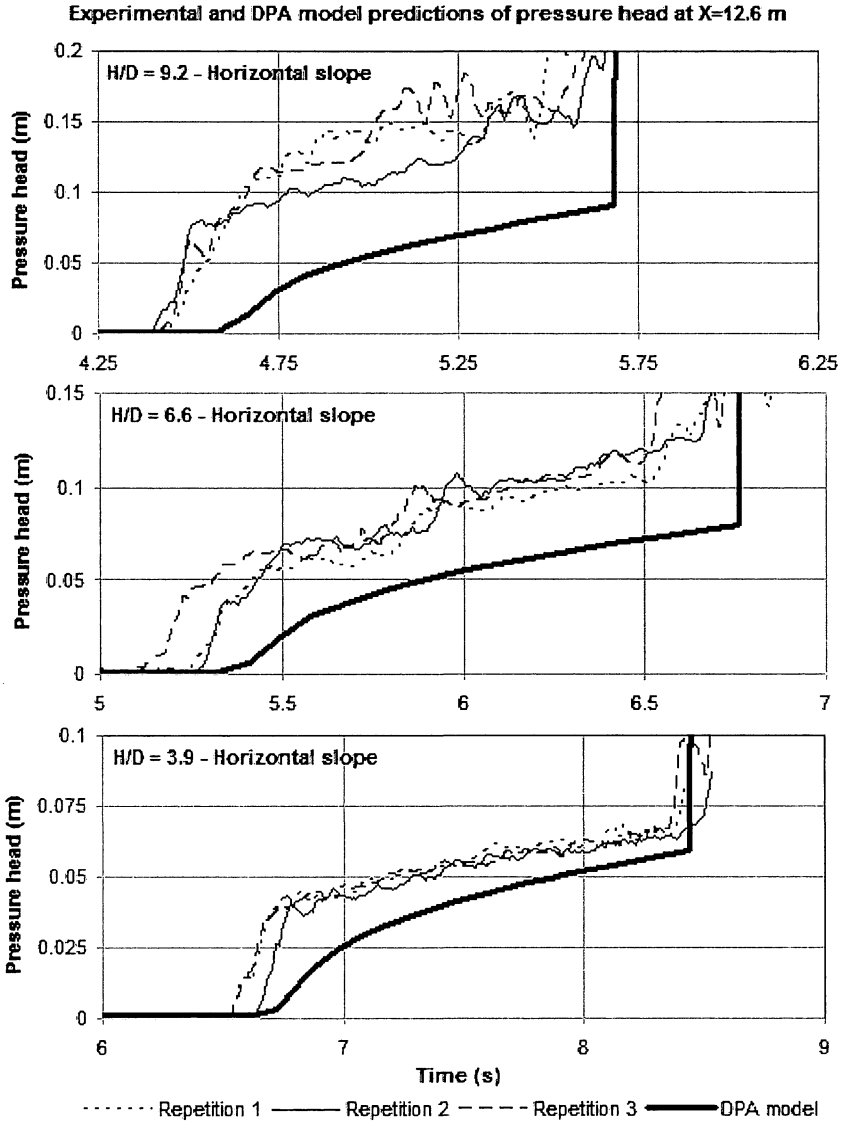

Figure 4.27: Pressure head measurements obtained with the transducer at the 12.6 m station for horizontal slope and numerical predictions from the DPA model.

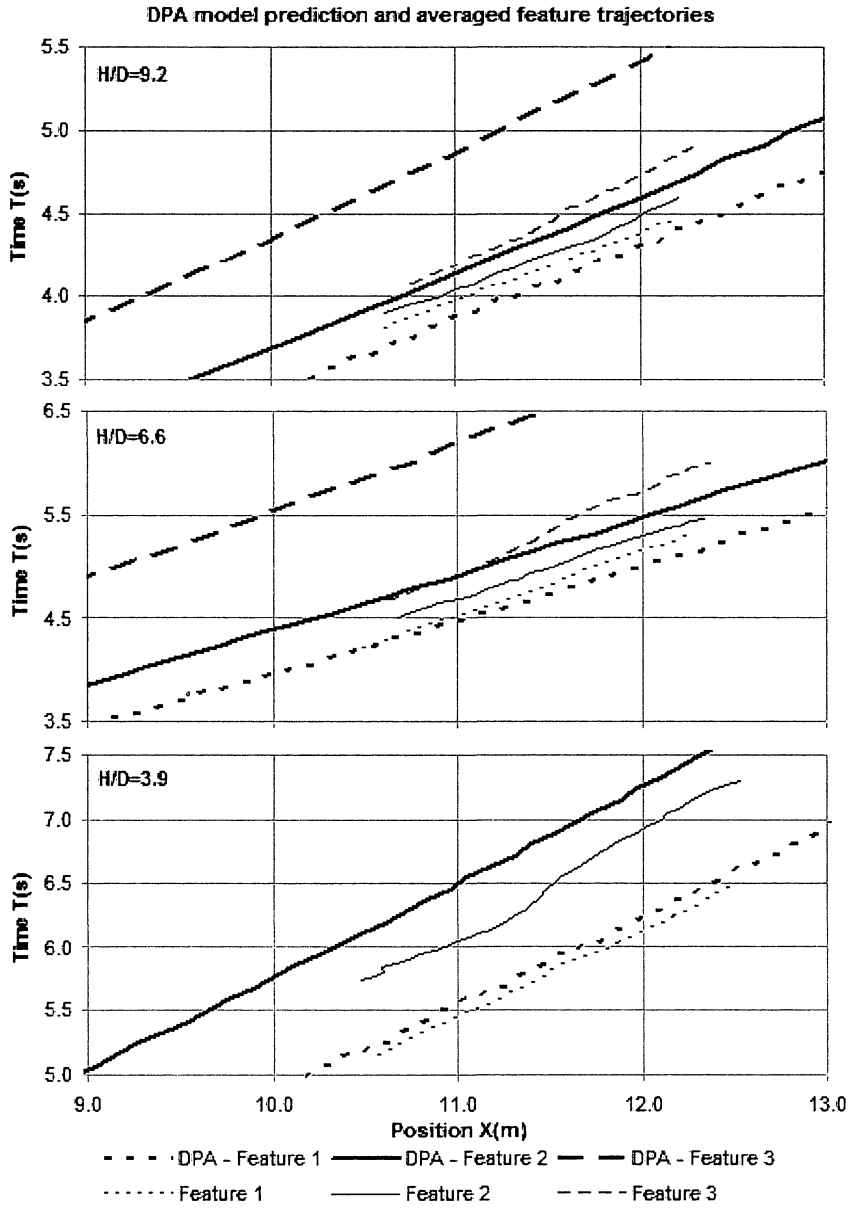

Figure 4.28: Comparison between the experimental measurement of the flow front trajectories and the front prediction from the DPA model.

4.5 Criteria for the an empty pipeline to flow full

As mentioned previously, there are at least two different mechanisms that determines whether a pipe flows full for a given inflow rate. The first criteria is based on the conveyance capacity of the pipe as an open-channel. If a given inflow exceeds the capacity of the pipe to flow in free surface flow conditions, pressurization will develop. The second criteria is based on a minimum velocity required to avoid a intrusion of an air cavity in the water flow.

From the observations in the experiments with regards to the velocity of the inflow front, it seems that the velocity based criteria is not adequate to determine whether the pipe flow will flow full. In the particular case of these experiments, the velocity based criteria would yield a required velocity of 0.52 m/s. Even in the lowest H/D ratio, the speed of the propagation front (assumed to be approximately similar to the flow velocity) is of at least three times this value. Yet, in most of these cases the observed flow was a free-surface flow at the front. It could be possible that the flow would become pressurized later on, but the pipeline length wasn't enough to have this confirmation. But for a larger velocity, above 1.8 m/s, the inflow front did fill the pipe cross section, although the front was spread over several pipe diameters with a width that appeared to increase with the propagation distance. These results indicate that the conveyance criteria is probably more adequate than the velocity criteria in determining whether the pipe will flow full or partially filled.

Chapter 5

Conclusions and Future Investigations

The objective of this report was to study the problem of the rapid filling of an initially empty pipeline. The experimental observations confirmed the complexity of this flow condition even in an idealized experimental apparatus such as the one used in this study. Nonetheless, some interesting conclusions resulted from this investigation:

- Some operational problems of the pipeline flow are related to the formation and entrapment of air pockets within the pipes during the filling process. These experimental results pointed to the occurrence of significant pressure oscillations caused by the expulsion of air pockets in ventilation points previously filled with water. Other operational problems, though possible, were not observed in these experiments;
- The shape of the pressurization front is very important in determining whether there is the possibility of air pocket formation. The experiments with lower H/D rations almost always yielded final configurations where air pockets where present;
- The assumption of vertical pressurization front is invalid in cases when the upstream pressure head is not too elevated. In the present experiments, H/D=3.9 generally resulted in free-surface flow conditions. Moreover, downward slopes (when pipeline slopes favorably to the flow) helped in the conveyance as a open-channel flow;
- Finally, the criteria to assure that the pipeline will flow full, thus avoiding the formation of air pockets behind the inflow front, should be based on the pipe conveyance rather than an intrusion velocity based criteria such as suggested by Liou and Hunt (1996).

Future experiments in this problem should include the following subjects:

- Measure the inflow front speed, including secondary velocities (transversal to the flow). This would help determine discrepancies from the idealized hydrostatic conditions used by numerical models such as the DPA model;
- Measure speed of the bulk flow;
- Use of a longer pipeline and longer experimental runs to assess whether an initially free-surface flow due to small H/D ratio would evolve into a pressurized flow;

- Use of two pressure transducers mounted on the top and the bottom of the pipeline to measure the over-pressurization of the flow;
- Use of different pipe slopes within the same run, particularly two segments with a low point in between to assess the air pocket formation due to water accumulation at those low points.

5.1 Acknowledgments

The authors would like to acknowledge the support of the CNPq, a Brazilian Government entity committed to the development of science and technology, which has provided a fellowship to support the PhD. studies of the first author.

Bibliography

Benjamin, T. B. (1968). "Gravity currents and related phenomena." *J. Fluid Mech.*, 31(2), 209–248.

Chow, V. T. (1973). *Open-Channel Hydraulics.* Civil Engineering Series. McGraw Hill, New York, international edition edition.

Izquierdo, J., Fuertes, J., Cabrera, E., Iglesias, P. L., and Garcia-Serra, J. (1999). "Pipeline start-up with entrapped air." *J. Hyd. Res.*, 37(5), 579–590.

Liou, C. P. and Hunt, W. A. (1996). "Filling of pipelines with undulating elevation profiles." *J. Hydr. Engrg.*, 122(10), 534–539.

Press, W. H., Flannery, B. P., Teukolsky, S. A., and Vetterling, W. T. (1989). *Numerical Recipes in Pascal.* Cambridge University Press.

Roe, P. L. (1981). "Approximate riemann solvers, parameter vectors, and difference schemes." *J. Comp. Physics*, 43, 357–372.

Townson, J. M. (1991). *Free-Surface Hydraulics.* Unwin Hyman, London, UK.

Vasconcelos, J. G., Wright, S. J., and Roe, P. L. (2005). "Decoupled pressure approach for the simulation of flow regime transition in sewers. Submitted to the Journal of Hydraulic Engineering.

Wisner, P. E., Mohsen, F. N., and Kouwen, N. (1975). "Removal of air from water lines by hydraulic means." *J. Hyd. Div. ASCE*, 101(HY2), 243–257.

Wylie, E. B. and Streeter, V. L. (1993). *Fluid Transients in Systems.* Prentice Hall, Upper Saddle River, NJ.

Yen, B. C. (2001). "Hydraulic of sewer systems." *Stormwater Collection Systems Design Handbook*, L. W. Mays, ed., McGraw Hill Handbooks, McGraw-Hill, New York, chapter 6.

Zhou, F., Hicks, F. E., and Steffler, P. M. (2002). "Transient flow in a rapidly filling horizontal pipe containing trapped air." *J. Hydr. Engrg.*, 128(6), 625–634.

Zukoski, E. E. (1966). "Influence of viscosity, surface tension, and inclination on motion of long bubbles in closed pipes." *J. Fluid Mech.*, 25(4), 821–837.

AIIM SCANNER TEST CHART # 2

Spectra

4 PT ABCDEFGHIJKLMNOPQRSTUVWXYZabcdefghijklmnopqrstuvwxyz:'',./?$0123456789

6 PT ABCDEFGHIJKLMNOPQRSTUVWXYZabcdefghijklmnopqrstuvwxyz;:'',./?$0123456789

8 PT ABCDEFGHIJKLMNOPQRSTUVWXYZabcdefghijklmnopqrstuvwxyz;:'',./?$0123456789

10 PT ABCDEFGHIJKLMNOPQRSTUVWXYZabcdefghijklmnopqrstuvwxyz;:'',./?$0123456789

Times Roman

4 PT ABCDEFGHIJKLMNOPQRSTUVWXYZabcdefghijklmnopqrstuvwxyz;:'',./?$0123456789

6 PT ABCDEFGHIJKLMNOPQRSTUVWXYZabcdefghijklmnopqrstuvwxyz;:'',./?$0123456789

8 PT ABCDEFGHIJKLMNOPQRSTUVWXYZabcdefghijklmnopqrstuvwxyz;:'',./?$0123456789

10 PT ABCDEFGHIJKLMNOPQRSTUVWXYZabcdefghijklmnopqrstuvwxyz;:'',./?$0123456789

Century Schoolbook Bold

4 PT **ABCDEFGHIJKLMNOPQRSTUVWXYZabcdefghijklmnopqrstuvwxyz;:'',./?$0123456789**

6 PT **ABCDEFGHIJKLMNOPQRSTUVWXYZabcdefghijklmnopqrstuvwxyz;:'',./?$0123456789**

8 PT **ABCDEFGHIJKLMNOPQRSTUVWXYZabcdefghijklmnopqrstuvwxyz;:'',./?$0123456789**

10 PT **ABCDEFGHIJKLMNOPQRSTUVWXYZabcdefghijklmnopqrstuvwxyz;:'',./?$0123456789**

News Gothic Bold Reversed

4 PT ABCDEFGHIJKLMNOPQRSTUVWXYZabcdefghijklmnopqrstuvwxyz;:'',./?$0123456789

6 PT ABCDEFGHIJKLMNOPQRSTUVWXYZabcdefghijklmnopqrstuvwxyz;:'',./?$0123456789

8 PT ABCDEFGHIJKLMNOPQRSTUVWXYZabcdefghijklmnopqrstuvwxyz;:'',./?$0123456789

10 PT ABCDEFGHIJKLMNOPQRSTUVWXYZabcdefghijklmnopqrstuvwxyz;:'',./?$0123456789

Bodoni Italic

4 PT ABCDEFGHIJKLMNOPQRSTUVWXYZabcdefghijklmnopqrstuvwxyz;:'',./?$0123456789

6 PT ABCDEFGHIJKLMNOPQRSTUVWXYZabcdefghijklmnopqrstuvwxyz;:'',./?$0123456789

8 PT ABCDEFGHIJKLMNOPQRSTUVWXYZabcdefghijklmnopqrstuvwxyz;:'',./?$0123456789

10 PT ABCDEFGHIJKLMNOPQRSTUVWXYZabcdefghijklmnopqrstuvwxyz;:'',./?$0123456789

Greek and Math Symbols

4 PT ΑΒΓΔΕΞΘΗΙΚΛΜΝΟΠΦΡΣΤΥΩΧΨΖαβγδεξθηικλμνοπφρστυωχψζ≧∓'',. / ≦±=≠°><⊁⊀⩾⩽≡

6 PT ΑΒΓΔΕΞΘΗΙΚΛΜΝΟΠΦΡΣΤΥΩΧΨΖαβγδεξθηικλμνοπφρστυωχψζ≧∓'',. / ≦±=≠°><⊁⊀⩾⩽≡

8 PT ΑΒΓΔΕΞΘΗΙΚΛΜΝΟΠΦΡΣΤΥΩΧΨΖαβγδεξθηικλμνοπφρστυωχψζ≧∓'',. / ≦±=≠°><⊁⊀⩾⩽≡

10 PT ΑΒΓΔΕΞΘΗΙΚΛΜΝΟΠΦΡΣΤΥΩΧΨΖαβγδεξθηικλμνοπφρστυωχψζ≧∓'',. / ≦±=≠°><⊁⊀⩾⩽≡

White

Black

Isolated Characters

e	m	1	2	3	a
4	5	6	7	o	°
8	9	0	h	I	B

A4 Page 6543210

MESH HALFTONE WEDGES

65

85

100

110

133

150

A4 Page 6543210

RIT ALPHANUMERIC RESOLUTION TEST OBJECT, RT-1-71

PRODUCED BY GRAPHIC ARTS RESEARCH CENTER

ROCHESTER INSTITUTE OF TECHNOLOGY, ONE LOMB

MEMORIAL DRIVE, ROCHESTER, NEW YORK 14623